RESEARCH REPORT

PHYSICS OF THE FIRST YEAR WITH ATLAS AT LHC

Pavel Jež

Supervisor: Václav Vrba

Acknowledgements

Declaration

I state that I wrote this report independently and exclusively with the use of cited bibliography.

Praha, 18th September 2007 Pavel Jež

Abstract

In the first chapter of this report, there is a brief overview of the contemporary state of the High-energy Physics. The emphasis is put on the validation of the Standard Model. One section is dedicated to the searches for Higgs boson(s), several production and detection mechanisms are introduced. Closing section of the first chapter then brings quick overview of the theories Beyond the Standard Model. Second chapter is dedicated to the description of the today's most promising particle collider LHC and and mainly to the state-of-the-art detector ATLAS and its subsystems. The special focus is on the Pixel detector. Next chapter is devoted to the ATLAS offline computing. The principles and using of the Athena - ATLAS offline software framework - are contained there. Last chapter covers student's own research activity: the effect of cosmic rays on the Pixel detector. This is done using Geant4 simulation within Athena. All the software tools are introduced and described, the preliminary results are then used to discuss their efficiency. Subsequently the cosmic rate and the distribution of hits and energy is estimated. Last section is outlook how to improve the cosmic rate estimate by folding in the trigger efficiency simulation.

Key words: Standard Model, ATLAS, pixel detector, cosmic rays, Athena.

Contents

Chapter 1

Questions of Contemporary Particle Physics

1.1 Overview of Standard Model

The Standard Model (SM) is our currently best describing model of the sub-atomic particles and their interactions. It was postulated during the end of 1960's and beginning of 1970's and since than it passed all experimental tests. Essentially, SM consists of a theory of weak and electromagnetic interactions (cf. [1]) and the theory of strong interactions (QCD - Quantum Chromodynamics - cf. [2], [3]). There are a lot of useful books and articles written about Standard Model (apart from [1–3], reader might wish to read [4] or [5]), here I decided to stress out only the main features of this theory.

The SM postulates that there are twelve elementary fermions which interact via twelve gauge bosons (cf. Tables 1.1 and 1.2). All this particles have been found (except from the Higgs boson, see below) and the predicted interactions were tested with the extraordinary precision (LEP collaboration, cf. [6]). Because the Standard Model is a quantum field theory, the particles are represented by fields or, more precisely, by their excitations. Details could be found in many QFT textbooks, e.g. [4,5].

The underlying symmetry group of Standard Model is $U(1)_Y \otimes SU(2)_L \otimes SU(3)_C$. This is an internal gauge symmetry, like in classical electromagnetism. Group $U(1)_Y$ comes from gauge transformations of electromagnetism, Y stands for (weak) hypercharge, i.e. twice the average charge of particle multiplets (see beyond). For example an electron has hypercharge -1, because it is in the same multiplet as neutrino. From the mathematical point of view, hypercharge tells us how the field transforms under $U(1)$ symmetry:

$$\Phi' = e^{iY\Lambda}\Phi \tag{1.1}$$

where Λ is arbitrary parameter. This symmetry is exact and unbroken, as far as we know.

Group $SU(3)_C$ comes from Quantum Chromodynamics, and C stands for color. There are three colors, so that the triplets are formed from the fields representing the same particle in different color variants. The field triplets form a fundamental representation of $SU(3)_C$. This symmetry is also exact and unbroken. The transformation looks like

$$\Phi' = e^{i\Lambda_j T_j}\Phi \tag{1.2}$$

where T_j are generators of corresponding group.

The last subgroup, $SU(2)_L$, could not stand alone. The field with such a symmetry (Yang-Mills field) has not been seen in nature yet. Nevertheless, the group $U(1)_Y \otimes SU(2)_L$ is the internal gauge symmetry of unified electromagnetic and weak interaction. The transformation

Table 1.1: Elementary fermions

		First generation	Second generation	Third generation	Electrical charge	Interaction
fermions	quarks	u-up	c-charm	t-top	+2/3	electromagnetic
		d-down	s-strange	b-bottom	-1/3	weak, strong
	leptons	e-electron	μ-muon	τ-tauon	-1	elmag., weak
		ν_e - e-neutrino	ν_μ - μ-neutrino	ν_τ - τ-neutrino	0	weak

Table 1.2: Elementary bosons

	Interaction mediated	Name	Spin	Electrical charge	Mass	Count
bosons	electroweak	$W^\pm$	1	± 1	80.4 GeV	2
		Z	1	0	91.2 GeV	1
		γ	1	0	0	1
	strong	g	1	0	0	8
	Higgs	H	0	0	≥ 114.4 GeV	1

of fields under this symmetry is the same as in (1.2), the only difference in in the matrices T_j. In case of the $SU(2)$ group the generators are Pauli matrices. Subscript L stands for left-handed, as only left-handed (i.e. spin vector points in opposite direction as the momentum vector) particles form non-trivial representation of $SU(2)$.

So that we have the lepton doublet formed by a lepton and corresponding neutrino, and the quark doublet formed by a up-type quark (u, c, t) and down-type (d, s, b) quark. Both of these doublets transform under $SU(2)$ as a fundamental representation, but they differ in transformation properties under $U(1)_Y$, as they have different hypercharge (cf. previous paragraphs). Right-handed particles form $SU(2)$ singlets. Contrary to previous symmetries, $SU(2)_L$ symmetry is spontaneously broken for the ground states. This means, that the ground state of a field symmetrical under group $U(1)_Y \otimes SU(2)_L$ possesses only $U(1)_Y$ symmetry.

We would construct the Lagrangian from the assumption that the transformations (1.1) and (1.2) are local for all three groups. Local in this case means dependent on the spacetime coordinate. This is a natural requirement to introduce gauge fields which represent gauge bosons (photons, W, Z, gluons), i.e. interactions [1]. The complete SM Lagrangian, which is invariant under Lorentz and local $U(1)_Y \otimes SU(2)_L \otimes SU(3)_C$ transformations is quite long [1], nevertheless it does not contain any mass terms - fermion mass terms ($\sim m(\overline{\psi}_L \psi_R + \overline{\psi}_R \psi_L)$) are forbidden by the symmetry, as left handed and right handed terms transform differently under $SU(2)_L$, and gauge boson mass terms spoil unitarity (i.e. if we introduce gauge boson mass terms, probability of particular process depends on when the process will take place).

The solution to this obvious discrepancy (fermions and some gauge bosons do have masses) is a spontaneous symmetry breaking of underlying gauge symmetry [1], as was already announced above. This is done by addition of scalar field which is invariant under complete symmetry, while its ground state ("vacuum") is not. This means we are introducing several scalar bosons. Their number depends on the degrees of freedom of that field.

Afterwards we suppose, that this field makes only small oscillations around its ground value and rewrite it in a form $\rho = \sigma + v$, where ρ is the original value, which was decomposed into small oscillations σ and vacuum expectation value v. There is a theorem saying that for each broken continuous symmetry we obtain a massless boson (called Goldstone boson, the procedure

is called Higgs mechanism). On the other hand, at least one scalar boson survives this process - and it is called the Higgs boson.

In case of Standard Model, we add a doublet of complex scalar fields (i.e. 4 spin 0 "particles") and we break the $SU(2)_L$ symmetry, which has 3 generators (Pauli matrices). Therefore we obtain 3 massless Goldstone bosons and 1 massive Higgs boson. However, the remaining $U(1)_Y$ invariance allows us to choose gauge (called U-gauge) in which all Goldstone bosons are identically zero, indicating that they are unphysical. The covariant derivatives were introduced by the $SU(2)_L \otimes U(1)_Y$ symmetry, therefore the added scalar fields are automatically coupled to the gauge fields. Thanks to the shift mentioned in previous paragraph ($\rho \rightarrow \sigma + v$), we obtain two types of terms: interaction ones and those, where the gauge field is coupled to the vacuum value. The latters are finally identified with the gauge boson mass terms, as the vacuum expectation value is just a number.

That is the way how gauge bosons obtain masses. Similarly, we can add masses to leptons: we add to the Lagrangian terms containing both leptons and scalar field doublet and that are invariant under all symmetries. When we come to the U-gauge, only Higgs boson and vacuum value remains (cf. previous paragraph) and we have lepton mass terms and lepton-Higgs interaction terms.

That is why the Higgs particle is really crucial in Standard Model - it is sometimes even called "golden particle". Regardless of its importance, and contrary to the other particles of Standard Model, it has not been spotted yet, so that its properties (and even its existence) are the most frequently asked questions of contemporary particle physics.

To be exact, not all fermion mass terms are forbidden - Majorana fermions (i.e. the particle is identical to its antiparticle) can have masses. However, because all fermions we can see are of Dirac type, this possibility was long disregarded. So that the only possible Majorana particles are left handed and right handed neutrino.

This particle was not included in the original Standard model which has exactly massless neutrino. Experiments of the past decade showed that this assumption is not true - neutrinos are slower than light, therefore they must have mass. On the other hand, they cannot be of Dirac type because we observe only left handed neutrino. The possible (and very elegant) solution is the introduction of superheavy right handed neutrino which mixes with the left handed one via the seesaw mechanism resulting in a tiny mass for the left handed neutrino.

Note that spontaneous symmetry breaking is not all-explaining (for example it cannot explain, why the masses of physical fermions range from almost zero (neutrino) to 170 GeV (top quark)), and contains some disturbing unrenormalizable divergences [7]. There are several extensions of Standard Model, which try to deal with these problems (the most well known is Supersymmetry), however in next section I will stick to the SM Higgs, because it is the simplest model and could be well used to explain the basics of Higgs phenomenology.

1.2 Higgs Hunting

1.2.1 How to discover a particle - HEP statistics

Before we will have a look on a particular experiments which tried or are trying to find Higgs boson, I would like to show what physicist have to do before they can claim discovery of a new particle.

Every collider experiment is based on measuring the energy of particles which were created in the beams collision. However, because our instruments are always imperfect, we are not able to measure the masses (energy, angles, momentum... etc.) of outgoing particles precisely. What we measure instead is some Gaussian distribution peaked at the value of the true mass of the particle. The standard deviation σ is decreasing with the number of events as $1/\sqrt{N}$. For

example when we are studying events like $e^+e^- \rightarrow W^+W^-$ and make a histogram of measured masses, we will find a peak at W mass.

If we find a mass peak in the region where it was not expected, we have (possibly) discovered a new particle. But sometimes an unexpected mass peak can be an error rather than a new particle. So that every new discovery should be made with at least 5σ significance. This means, that there there is only 0.000006 % probability, that the signal was due to statistical fluctuation of the background. The Fig. 1.1 shows the example of Higgs signal together with possible background at CDF at Tevatron.

If we want to find Higgs boson, we have to answer two principal questions - how to produce it and how to detect it. Naturally, answers differs from machine to machine, so let's have a look at three most important of them: one that was, one that is, and one that will be.
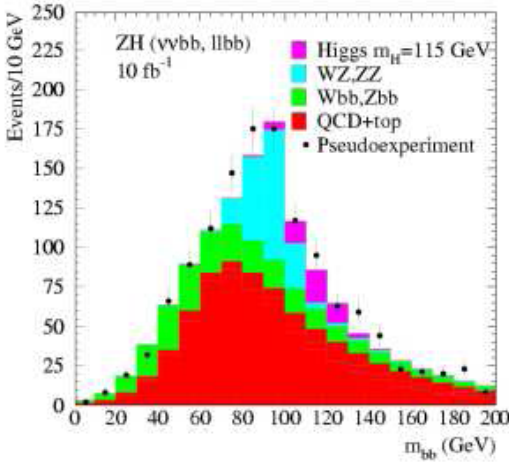
Figure 1.1: Higgs signal in the invariant mass of $b\bar{b}$ pairs at CDF, Tevatron. Figure from [8].
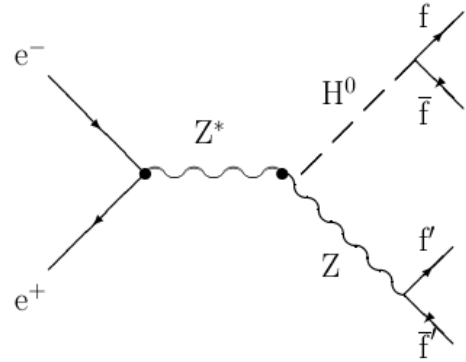
Figure 1.2: Higgs boson production via Z boson. Figure from [8].

1.2.2   LEP

Large **E**lectron-**P**ositron collider was in operation in CERN from 1989 until 2000. Electrons and positrons were accelerated to the energy of 45 GeV (LEP I), enabling production of Z boson (its mass is approx. 91 GeV) and the energy was further increased (LEP II), until it topped 104 GeV in 2000, long before enabling production of W pair (W mass is approx 80 GeV). So, what are (according to Standard Model) the main production mechanisms of Higgs boson in this environment?

Higgs couples to all massive particles and the strength of coupling is proportional to particle mass. Therefore, the Higgs boson most likely appears in decay of heaviest particles - Z and W bosons. Note that direct production of one Higgs particle in electron-positron collision would have taken ca. 4 years [8] of LEP running at full luminosity and energy. The LEP focused on process $e^+e^- \longrightarrow ZH$ (see Fig. 1.2), because it had much wider mass window for Higgs than the process $e^+e^- \longrightarrow W^+W^-H$.

We know very well decay channels of Z boson (mostly to jets, 20 % of time to neutrinos and 10 % of time to fermion-antifermion pairs). But what are the decay products of the Higgs particle? It is a neutral boson, coupled to all massive particles, so that it decays to fermion-antifermion pairs, W^+W^- or ZZ pairs. Strangely enough, the Higgs has also massless final

products emerging in loops as direct coupling is not kinematically allowed. Photons can be produced in heavy quark loops, as well as W loops. Color carrying gluons may originate only from heavy quark loops.

Decay rates may be calculated using standard methods of Feynman diagrams and are of course highly dependent on yet-unknown mass of Higgs boson. The plot of branching ratios is on Fig. 1.3)
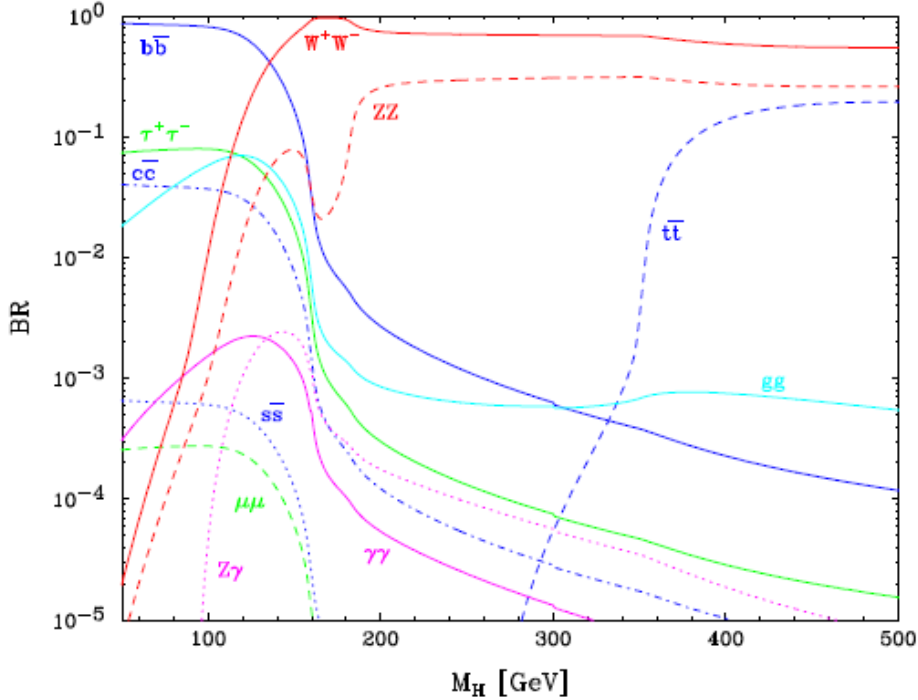
Figure 1.3: Branching ratios of selected SM Higgs decays at LEP as a function of Higgs mass. Figure from [8].

This was the theory, so how to actually detect, that the Higgs was present in an event? Quick glance at masses and energies of e^+e^- beams tells us that LEP was not able to produce Higgs with higher mass than ~ 113 GeV in ZH events. Therefore the dominant decay channel of Higgs at LEP was the decay to $b\bar{b}$ pair.

Bottom quarks are unstable and decay before they can reach some detecting device. However, their lifetime is long enough to travel significant distance from the interaction point (primary vertex in HEP jargon) and then decay in the secondary vertex. This property, together with the fact that b-meson is much more heavier than anything it can decay into makes bottom quarks well identifiable.

The background for the Higgs production comes from the direct interaction of electron and positron beams. Because leptons can interact only by electroweak interaction (and Higgs as well), the background and signal rates are roughly the same. That means all possible decay channels were studied.

The most promising was the largest one: $ZH \to b\bar{b}jj$. However, also the channels with lower decay rate could have been interesting. For example $ZH \to b\bar{b}\ell\bar{\ell}$. This event has ca. 6 times lower branching ratio than decay to jets, however, because leptons can be identified much more precisely than jets, a smaller sample of such an events would have had the same significance of signal over background as the larger sample of $ZH \to b\bar{b}jj$.
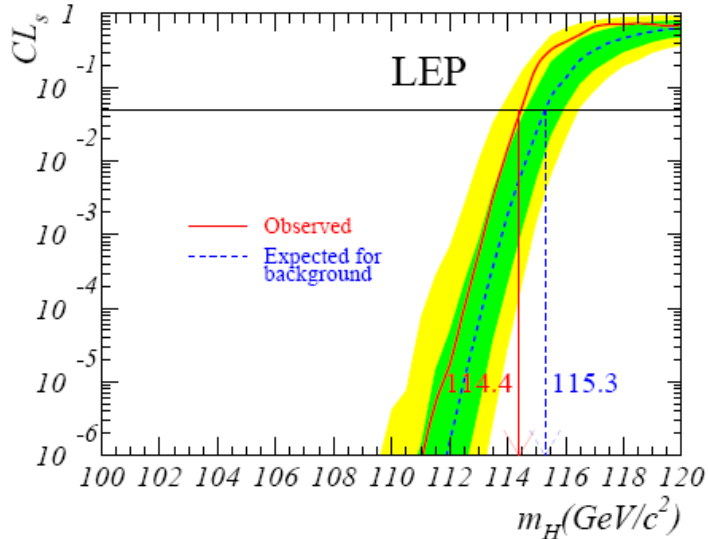
Figure 1.4: Lower limit on a Higgs mass from combined data from 4 LEP experiments. It shows the confidence level (cf. text) as a function of the Higgs mass. Blue dashed line are values expected from the theory, red line is actual experimental result. Its position implies that they have actually seen more events in the 114 - 116 GeV mass bin than they had previously thought. Figure from [8].

Nevertheless, LEP collaboration was unable to see any Higgs signal. The result of their search is on Fig. 1.4. Only at the end of LEP run, there were a few Higgs-like events (see Fig. 1.5), but their significance over expected background was only some 2 σ's, too few to claim a discovery. But it was enough to set a lower mass limit of 114.4 GeV with 95 % confidence (i.e. the probability that they have seen Higgs of this mass or lighter and have not discriminated it from the background is less than five per cent)

1.2.3 Tevatron

Tevatron is current largest particle accelerator, built in Fermi National Accelerator Laboratory in the United States. At the end of the 1990s it was upgraded to the energy 1.96 TeV and also the luminosity was increased. So theoretically, Tevatron could produce Higgs boson with masses up to 1.96 TeV, but the cross-section for heavy Higgs mass production is so small, that the practical mass range is not much higher than the one at LEP. The reason for this is large QCD background coming from the proton-antiproton collisions.

Similarly to the LEP, producing Higgs directly in $p\bar{p}$ interaction is hopeless task, so that here they also try to produce Higgs coupled to some heavy particle. While LEP specialized essentially in one production channel, Tevatron will have more possibilities. The first is essentially the same as before - quark-antiquark annihilation to create the W boson, which scatters away and produce Higgs boson (fig. 1.6 c). Also, the energy range allows top quark loop, so that Higgs is coupled to the $t\bar{t}$ quark pair - the heaviest known elementary particle (fig. 1.6 a).

But the Tevatron energy range allows even more: top quark from the loop can come on-shell and the Higgs is produced together with the top-antitop pair (fig. 1.6 d). Thanks to that, it is an event with a very distinct topology.
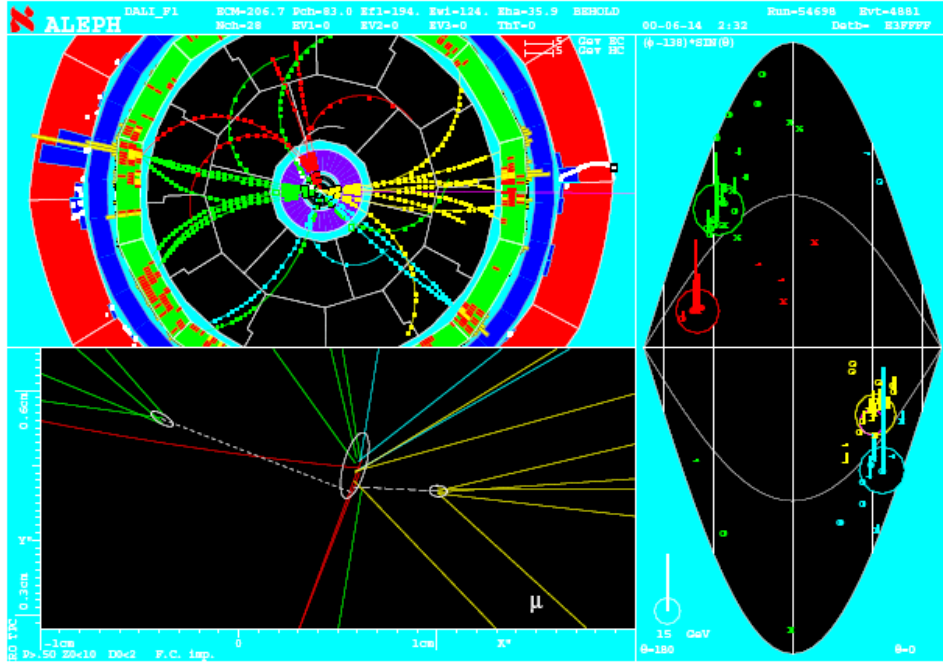
Figure 1.5: Event display of one of the Higgs candidates at LEP. The possible explanation for this Figure is Higgs decaying into $b\bar{b}$ - this is symbolized by yellow and green jets - and Z decaying into 2 jets. These are red and blue. Figure from [8].

Last major type of Higgs production is also topologically interesting: it is so-called weak boson fusion (WBF) and means that incoming quarks emit W or Z boson which fuse to create the Higgs boson. The cross-sections of various production processes is in Fig. 1.7.

Comparing Figures 1.3 and 1.7 we may think that the "golden channel" would be $gg \rightarrow H \rightarrow b\bar{b}$. However, the background from $p\bar{p} \rightarrow b\bar{b}$ is many orders of magnitude higher than the signal [8].

We can avoid large QCD background by demanding that we will have at least one high-energy lepton in the final state. This is the typicall trigger of hadron colliders. Such a particle could be produced only via W and Z boson, meaning that (at least part of) the interaction was electroweak, or via top quark which is produced less frequently than other particles.

In practice it means that Tevatron searches are focused on Higgses created by Higgsstrahlung (1.6 c, i.e. in principle the same as in the case of LEP) and then decaying into $b\bar{b}$ pair in case of a light Higgs (≤ 140 GeV).

In case of heavier Higgs boson it is more perspective to look for decays to the W^+W^- pair, produced either by gluon fusion (1.6 a) - this has the highest production rate - or by Higgsstrahlung, which is, on the other hand, better distinguishable from the background.

As of summer 2007, there is no reported discovery on any of these channels. The chances are highly dependent on the Tevatron event rate and of course on the Higgs mass. Figure 1.8 shows how big amount of data will be needed to make a discovery, or at least to exlude another mass region. Now, the amount of analyzed data is slightly more than 1 fb^{-1}

1.2.4 LHC

The **L**arge **H**adron **C**ollider is just being finished in CERN. It is being built in the old LEP tunnel. Unlike LEP, it will be a hadron collider, and unlike Tevatron, it will be a pp collider. The projected energy of each beam is 7 TeV, and the full luminosity in the first phase of LHC
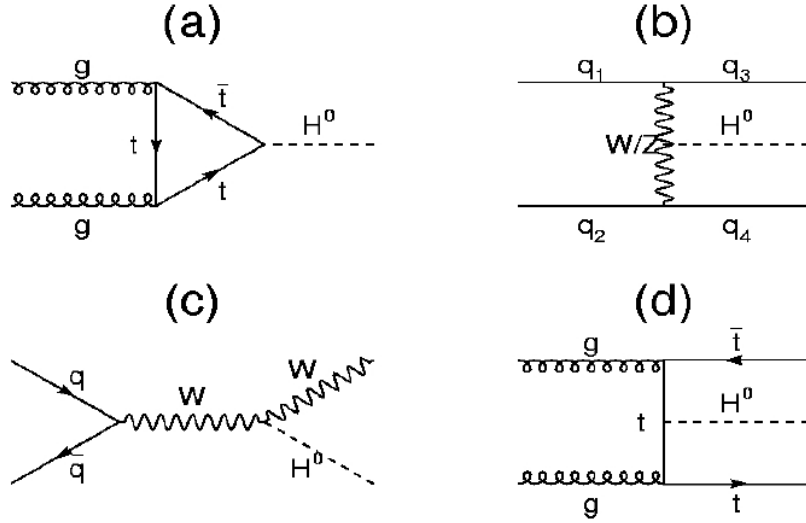
Figure 1.6: Dominant Higgs production in the hadron collider. Figure from [8].

run would be 10^{34}cm^{-2}s^{-1}. Around 2015 the upgrade to Super LHC (SLHC) is planned. This means that the luminosity would be further increased by a factor of ten. However, it is possible that also the energy will be increased, as the discussions are still ongoing.

The unprecedented luminosity of LHC (it is 100 to 1000 times higher than at the Tevatron) is achieved by the very dense beams: the proton bunches are separated by approx. 25 ns and contain 10^{11} particles resulting in around 800 millions of collisions per second (ca. 20 collisions per bunch crossing).

In principle, the Higgs physics at LHC will be similar to that at Tevatron. But thanks to the larger energy, the cross-section of Higgs production will not be negligible even for heavy Higgs. Figure 1.9 shows cross-section for various processes at LHC. We can see, that Higgs production will be dominated by gluon fusion, while Higgsstrahlung will be several orders of magnitude smaller.

The dominant background will come, as in case of Tevatron, from the QCD processes. Their cross-section at LHC will be also larger than at the Tevatron and, for example, the channel with highest rate ($gg \rightarrow H \rightarrow b\bar{b}$) will still be useless.

Nevertheless, because the cross-sections of the production of electroweak gauge bosons rises more slowly than the QCD-like $gg \rightarrow H$ the processes like $gg \rightarrow H \rightarrow W^+W^-$ will be quite promising. On the other hand, one of the main channels at Tevatron and the main channel at LEP, i.e., the Higgs is produced together with some weak gauge boson, will be useless because of high background from $pp \rightarrow Wb\bar{b}$ and $pp \rightarrow Zb\bar{b}$

In general, the Higgs production rate during the LHC run (at least tens of thousands in case of Standard Model Higgs) allows serious study of rare channels like production via weak boson fusion (fig. 1.6 b) or top-antitop associated production (fig. 1.6 a). These channels have distinctive topology, so that we have good reason to believe, that they will play important role in the LHC Higgs search.

Let's examine this processes in more detail. The schema of $t\bar{t}H$ associated production and subsequent decay is described by a diagram given in Figure 1.10. The backgrounds for this signal are QCD processes $t\bar{t}b\bar{b}$ and $t\bar{t}jj$. In the earlier studies these backgrounds were calculated using the soft approximation for the extra (b) jets (i.e. these mimicking the Higgs decay), although these jets should be very energetic - the particle with mass larger than 100 GeV decays into something which has mass of about 8 GeV at maximum. Such an inappropriate approximation

14
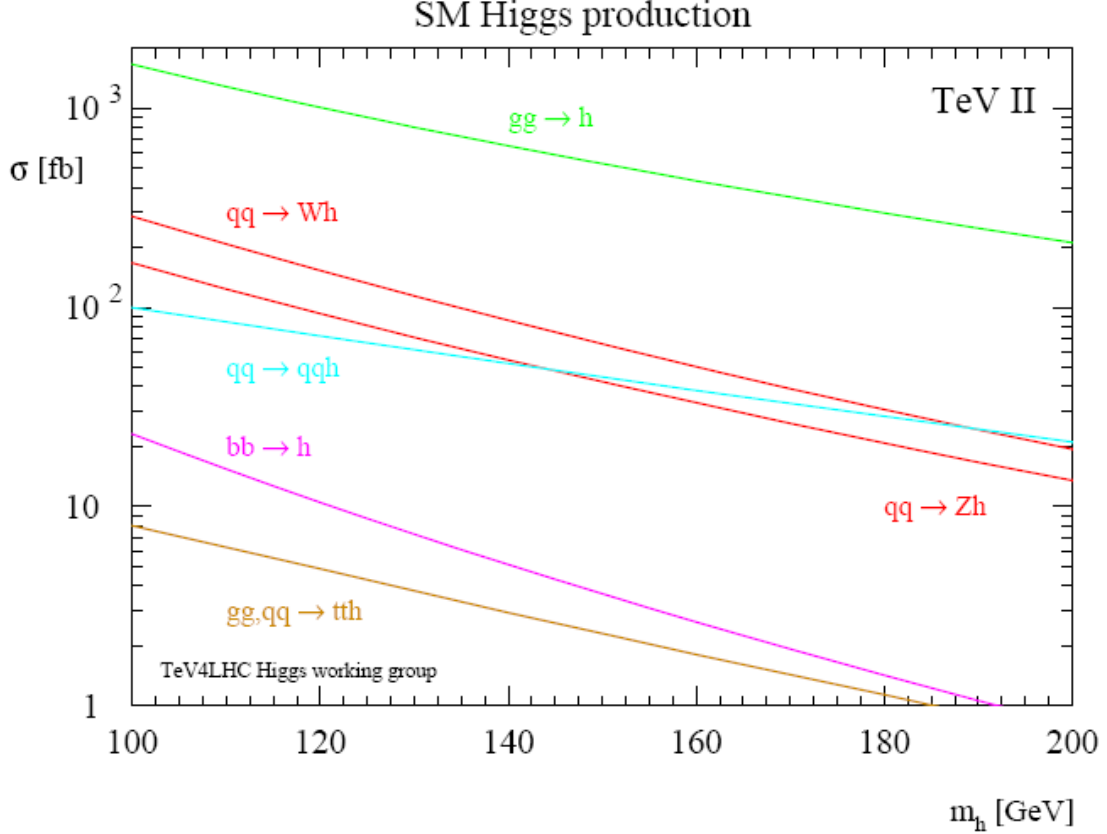
Figure 1.7: Cross section of various SM Higgs production processes at Tevatron Run II. Figure from [8].

lead to the underestimation of the background rate. When using proper calculation [9], we would get something like Figure 1.11.

The first thing one can see on this plot is quite poor signal over background ratio. In this case it is about 1/6. However, thanks to the large LHC statistics, this should not be critical. The problem lies somewhere else.

As it was mentioned earlier in the previous section, to claim a discovery, a signal associated to a new particle must be found with a 5σ significance. This requires both precise measurement (this gives signal + background) *and* precise knowledge of the background. In this case the second demand causes the problem. Due to uncertainty in Monte Carlo jet production, the overall uncertainty of the shape of the background (denoted usually as Δ) is approx. 10 %.

The formula for channel significance than becomes

$$\frac{S}{\sqrt{B}} \longrightarrow \frac{S}{\sqrt{B(1 + B\Delta^2)}}$$

where S stands for signal and B for background. Even if we have infinite statistics (i.e. $S \rightarrow \infty$ and $B \rightarrow \infty$), the significance will become constant:

$$\frac{S/B}{\Delta}$$

.

15
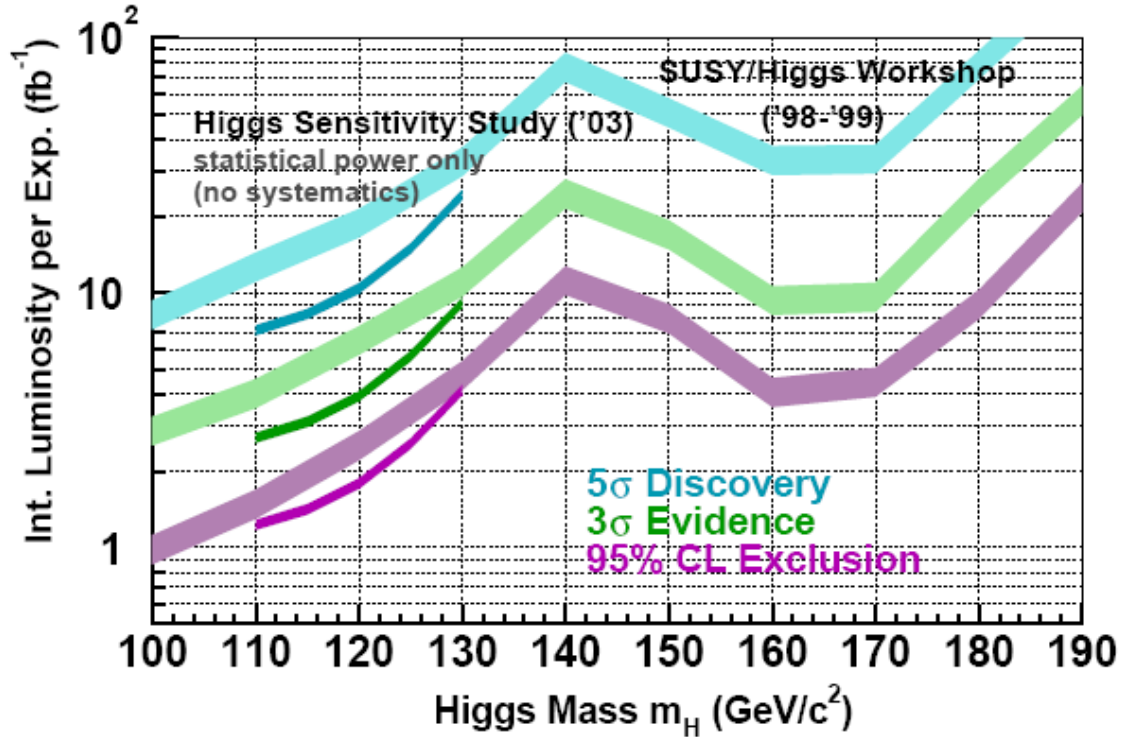
Figure 1.8: The amount of data needed at Tevatron Run II to discover or exclude Higgs as a function of its mass. Figure from [8].

Numerator and denominator of this expression are constants, so for the case of $t\bar{t}H$ events the significance cannot be better than 3σ's, unless our knowledge of the shape of the background improves.

This could be done by some next-to-leading order QCD calculation, which will probably take several years. So for the time being the $t\bar{t}H$ channel will certainly not be useful for discoveries, although it might give some information about couplings.

Now, lets turn our attention to the other complex production channel: the weak boson fusion. Due to its low rate it is not of any use at Tevatron, but at LHC the situation is quite different. The cross-section of weak boson fusion is about an order of magnitude smaller than the cross-section of the production via gluon fusion, but it still gives very nice event rate. Of course it depends on the Higgs mass, but even for the heaviest SM Higgs scenarios we would get many thousands of events during the LHC operation.

This production channel has very distinctive kinematics which makes it easy to suppress the backgrounds and consequently come to the result with high statistical significance. The scheme of WBF is repeated on the Figure 1.12. This picture also shows typical outcome of this event, which are the jets coming from the scattered quarks and jets coming from the Higgs decay. What makes this channel so interesting is the position of these jets.

The quark jets are scattered far forward and far backward, respectively, so they are called the tagging jets. The reason is that the more 4-momentum passes from the incoming quark to the W or Z boson, the less probable this process is. Therefore the quarks change their 4-momentum as less as possible leading to small scattering angles, which means large pseudorapidity. Higgs decay products then stay in the central area.

Other distinctive feature is the QCD radiation which is completely different from the radiation coming out of QCD production processes. At WBF it is scattered at small angles, creating

16
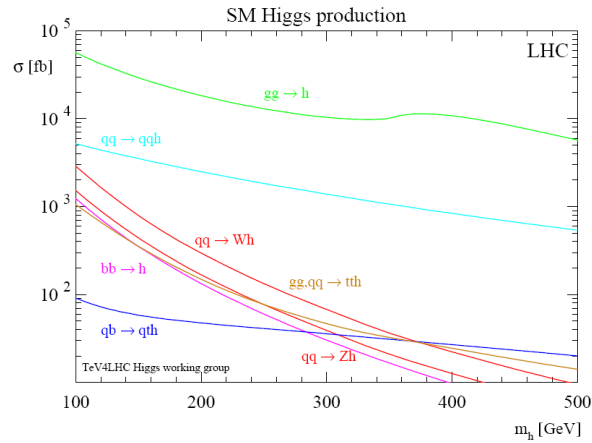
Figure 1.9: Cross section of various SM Higgs production channels at LHC as a function of Higgs boson mass. Figure from [8].
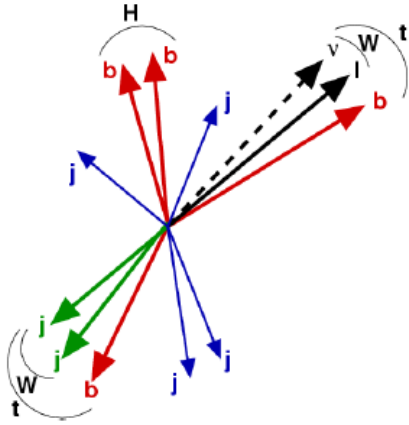
Figure 1.10: The scheme of $t\bar{t}H$ associated production and subsequent decay. Figure from [8].
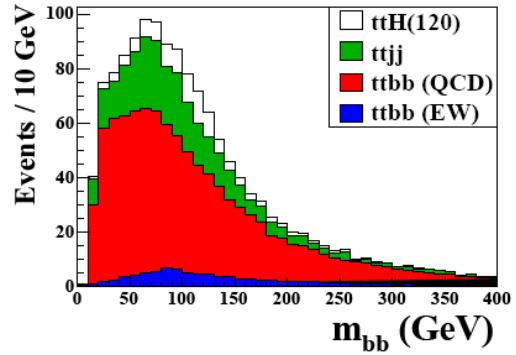
Figure 1.11: Recent result for the $t\bar{t}H \to b\bar{b}$ channel. Figure from [8].

the forward and backward jets while at QCD production, we have jets in central region. If we place a veto on a central jet, demand far forward/backward jets and expect Higgs decay products in the central region, we will eventually obtain a very clean signal. The comparison of WBF signal and QCD background is on Fig. 1.13.

The next question is, which decay products should we be looking for. If we look for light Higgs (≤ 130 GeV), the largest rate has $H \to \bar{b}b$, but the QCD background is several orders of magnitude higher than the signal. The next to largest rate is decay to $\tau^+\tau^-$, which fortunately has more EW than QCD background. Dominant background is Zjj production, which is, unlike the ttH case fairly well understood, so we do not have to worry about shape uncertainties and statistical significance limit.

Joint ATLAS and CMS study [10] found that this channel would be extremely promising, cf. Figure 1.14. The mass resolution should be a few GeV even with a relatively small amount of data and without the central jet veto.

If the Higgs mass would be greater than 140 GeV, the decay to W pair would become dominant mode. This is very promising, because it has much lower background than the $H \to b\bar{b}$
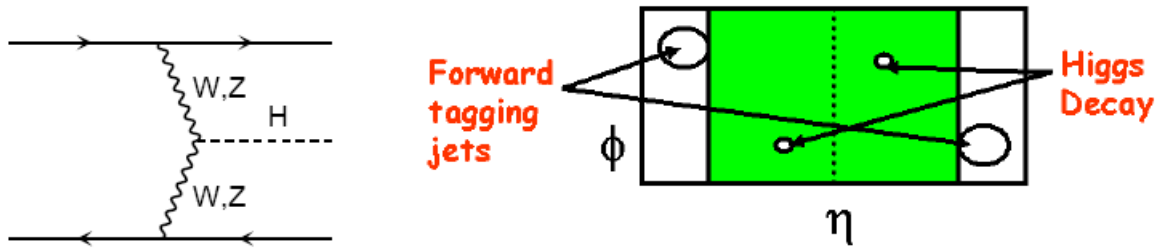
Figure 1.12: The scheme of weak boson fusion. On right there is lego plot showing very distinctive signature of this production channel. Figure from [8].
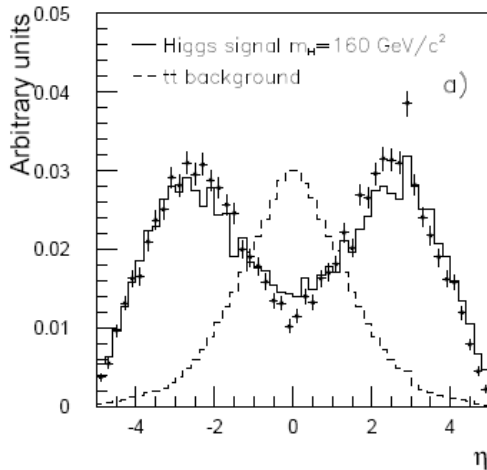
Figure 1.13: Pseudorapidity of jets during weak boson fusion. Large separation of signal and background is clearly visible. Figure from [8].
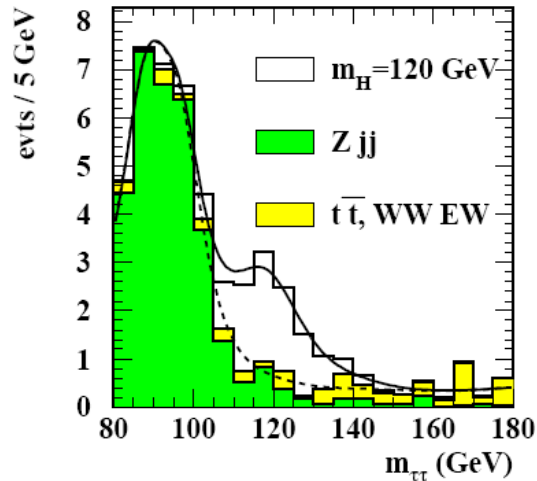
Figure 1.14: Simulation of WBF produced Higgs decaying into $\tau^+\tau^-$ pair on ATLAS for 30 fb^{-1}. Figure from [10].

decay. Figure 1.15 shows the results from already mentioned study [10] for this channel. Signal over background ratio is bigger than one for Higgs ≥ 140 GeV, and is still quite good for the values close to the LEP experimental limit.

Decay into W pair can also make top associated Higgs production useful. The backgroud is now mixed QCD and EW, making it easier to predict, calculate and simulate than the pure QCD like in the decay into $b\bar{b}$. A nice feature of this channel is, that while the $t\bar{t}H$ cross-section falls with the rising Higgs mass, the branching ratio of decay into W pair rises. Therefore we would have more or less constant event rate over the large spectrum of possible Higgs masses.

To sum up this section, there are several possible ways to discover Higgs, all of them will be used in some way at LHC experiments. Then there are several other channels, which cannot be directly used for discovery, either due to uncertain background ($t\bar{t}H \rightarrow b\bar{b}$) or due to low rate (generally all channels including decays $H \rightarrow \gamma\gamma$). On the other hand, they can be used for measuring Higgs couplings. The most promising channel seems to be weak boson fusion production due to its decent rate and very distinctive kinematics and therefore low background. Figure 1.16 shows the statistical significances of various channels as the function of Higgs mass.
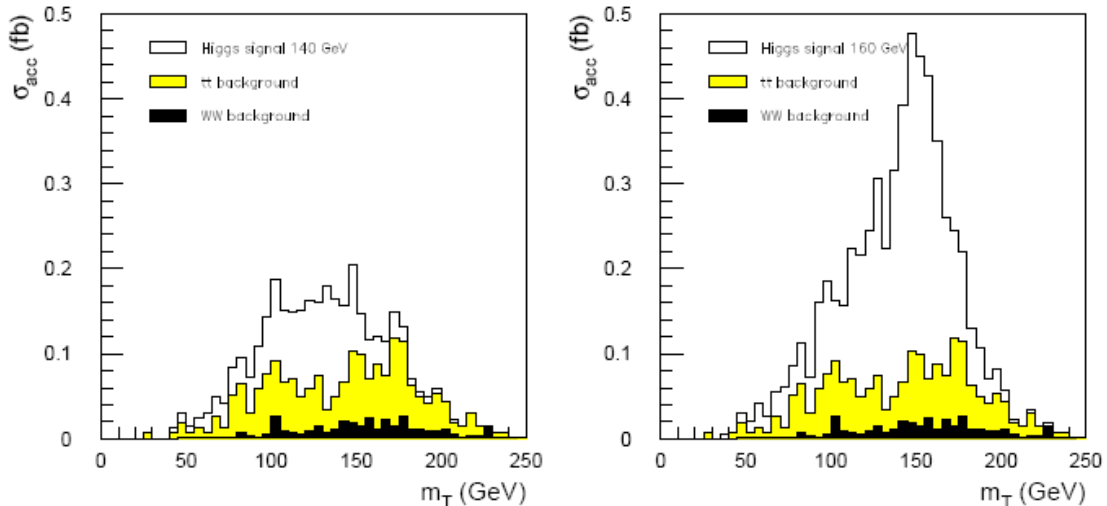
Figure 1.15: Simulation of WBF produced Higgs decaying into $W^{\pm}$ pair for two different Higgs masses and for for 30 fb^{-1} of data. Figure from [10].

1.3 Beyond the Standard Model

Last section showed some properties of the SM Higgs phenomenology. If it were found either at Tevatron or at LHC in the way described in that section, than we would have a good reason to believe that Standard Model is meaningful theory of the subatomic world. But it may happen that there is no Higgs particle at all. This would imply that particles acquire masses by some other mechanism. In fact, theorists proposed several other mechanisms how particles can become massive, but the SM Higgs mechanism is by far the simplest of them.

The most well known of the non-Higgs mechanisms are the technicolor models. They suppose that there are other fermions beside these predicted by the SM and that the SM gauge group is embedded in a larger symmetry group which spontaneously breaks down to the Standard model group. The simplest technicolor models have been already ruled out by precise electroweak measurements.

It can also happen that the Higgs particle exist, but we would not be able to see it. The models with "hidden" Higgs are embarassingly simple, they are only slight modification of the Standard model. The basic idea is, that the Higgs potential contains also phantom scalar field which does not interact in any way with the other fields of the SM. The Higgs mass eigenstates are then inevitable mixtures of the "normal" scalar Higgs field and this phantom field.

In the experimental situation this means that instead of having e.g. one signal with significance 2 σ's, we would get 2 signals with significance 1 σ. So, in fact, the discovery would require twice as presice measurements and background knowledge than we would need in case of pure SM Higgs.

Quick glance at Figure 1.16 now reveals that only two channels could claim discovery and only in a narrow mass window. But imagine, that we have two or more phantom fields. In this case we would not be able to measure any Higgs signal. More details about hidden Higgs model could be found in talk of F. Wilczek [11].

On the other hand, if we find Higgs and its mass and couplings would match all the predictions, we would not be finished. In contrary, the existence of Higgs would finish the validation of the Standard Model and we are almost certain that although the Standard Model is internally consistent, it is not the final theory. There are various aesthetical reasons like big numbers of free parameters, but also some questions the SM is not able to answer in satisfactory way.
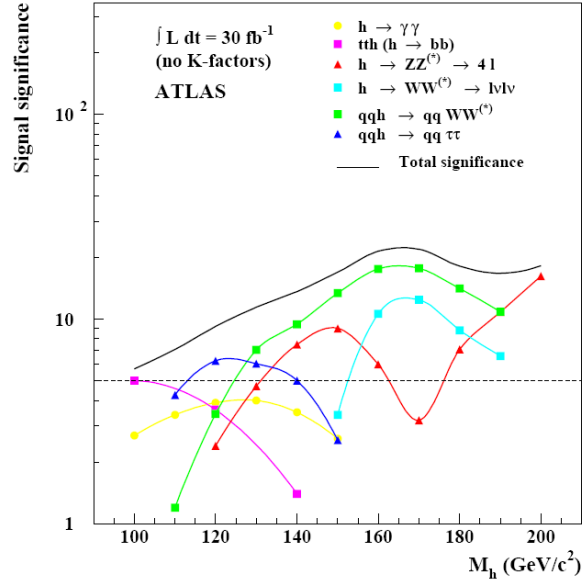
Figure 1.16: Statistical significance of the various discovery channels at ATLAS for 30 fb^{-1} of data. Figure from [8].

The problems arise for example in the Higgs sector. We know that $U(1)$ symmetry of electromagnetism protects photon self-energy diagrams from blowing up at high energies. Similar is true for the electron self-energy - it is protected by chiral symmetry. Because this symmetry is not exact (electron is massive particle - it is exact for $m_e = 0$), there is a logarithmic divergence, which is, however, proportional to the electron mass, so it could be handled without much problems.

Nevertheless, there is no symmetry to protect Higgs self-energy diagrams from blowing up at infinity. The divergence is in this case proportional to the scale of the theory squared. This means, that if we want to maintain Higgs mass at the order of hundreds GeV, we will have to add counterterm 30 orders of magnitude larger than Higgs mass. This correction would be also different in different orders of perturbation theory.

This is very disturbing and it was called the Hierarchy problem. Solution is to bring another symmetry which will protect scalar masses like electromagnetism and chirality protects photon and fermion masses. The new symmetry is called Supersymmetry and basically it is a symmetry between fermions and bosons. More details are in the next section.

Other problems of the Standard Model lies in the flavour sector. As was already mentioned, experimentalists found that contrary to SM prediction, the neutrinos have masses. Consequence of this is neutrino mixing, i.e. neutrino changing its type from electron to muon or tauon during its lifetime. The transition probability is quite well measurable and is dependent on the mass difference.

This could be implemented to the Standard model by addition of massive right handed neutrinos which give masses to the light left handed neutrinos through seesaw mechanism.

Since we have managed to unify electricity and magnetism and the electromagnetism with weak interactions, the natural question is, whether it is possible to unify electroweak and strong forces? Generally the unified theory is called Grand Unified Theory (GUT) and would mean, that both Standard Model and QCD gauge symmetry groups would be included into one larger group. There is a lot of proposal, the most simple of them (group $SU(5)$) has been ruled out, because it predicted too short lifetime of a proton.

More elaborate GUT's have problems with too many dimensions. For example the simplest

Higgs representation in the largest exceptional group E_8 has more than 3000 dimensions.

One aspect of GUT's is the unification of coupling constants. This seems plausible, because the coupling constants are running and while the strong coupling is still smaller for larger energies, weak and electromagnetic coupling increases. However, this three lines does not meet in a point, unless we suppose something similar to Supersymmetry.

Other challenges come from the cosmology - it is the existence of huge amounts of non-baryonic matter in the universe (96 % of all energy). This could be partially described by the supersymmetric particles (dark matter - see below), but still there is a problem with dark energy.

Standard model also does not explain, why we cannot see the free quarks and whether they have some structure.

Ultimate question is the implementation of gravity - most popular in this case is the super-string theory, which suppose that the basic objects are not pointlike particles, but rather 1D objects called strings. Note that to obtain some physical meaning, the introduction of super-symmetry to the world of strings is practically compulsory.

These are the main questions the Standard Model is not able to answer. So that a lot of theories which go 'beyond the Standard Model' were developed in past years. Mostly, they solve some problematic part in the Standard Model, but, on the other hand, quite often they bring other questions. The problem now is to choose which of these theories (if any) is true. Their predictions are different from each other and also from the Standard Model only for higher energies we have not been able to reach so far. With LHC we would be able to explore completely new region of TeV energies. It is widely expected, that LHC will give us a clue which of the BSM theories is right.

1.3.1 SUSY

The most well known beyond the SM theory is Supersymmetry. As was already mentioned, basic aim was to cancel quadratic divergences in the Higgs sector. The divergences are coming from Higgs self-energy diagrams, i.e. fermion loops. Their contribution can be canceled if there would be some symmetry between bosons and fermions. Because we do not see such a symmetry, this would force us to introduce new bosons which will cancel the loop contributions of fermions in Higgs self-energy.

This is the basic idea behind Supersymmetry. How to apply it? The symmetries of Minkowski spacetime form Poincare group. This means 3 translations, 3 rotations and 4 Lorentz boosts. Each symmetry has its generator and this ten generators together form the Poincare algebra. It is defined by the commutation relations between the generators of symmetries.

We know that there are also other symmetries like internal (gauge) symmetries of the Standard model. However, Coleman-Mandula theorem [12] states that it is impossible to combine space-time and internal symmetries in any but trivial way (i.e. the result is tensor product of Poincare group and the added internal symmetry). By non-trivial combination they mean that there exist some non-zero commutators between the generators of the Poincare group and the internal symmetry.

Therefore, to add new symmetry to our field theory, we have to set some *anticommutators*. The simplest case is to add just one supersymmetrical generator, let's denote it Q. Because it should change fermions into bosons and viceversa, it has to have spin 1/2 - so that it is fermionic field. The generator is a 2-component Weyl spinor. Its conjugate is operator $\overline{Q}$. The anticommutors of generator of supersymmetry and generator of momentum are

$$\{Q_\alpha, Q_\beta\} = \{\overline{Q}_{\dot\alpha}, \overline{Q}_{\dot\beta}\} = 0 \qquad \{Q_\alpha, \overline{Q}_{\dot\beta}\} = 2\sigma^\mu_{\alpha\dot\beta}P_\mu$$

All commutation relations between the supersymmetry generators and the Poincare group generators are zero. The indeces $\alpha, \dot\alpha$ run from 1 to 2 and σ^μ is formed from Pauli matrices:

$\sigma^\mu = (1, \sigma^i)$. So we see that generators of supersymmetry have fermionic properties: they anticommute. Because of that we have to introduce new spacetime variables, called Grassman variables. They are basically the numbers which anticommute with each other and we denote them as $\theta, \overline{\theta}$.

Now we can define the finite supersymmetrical transformation. The normal spacetime translation is

$$p^\mu = e^{-ix_\mu P^\mu}$$

So that the supersymmetrical spacetime finite transformation is

$$p^\mu = \exp i[(\theta Q + \overline{\theta Q} - x_\mu P^\mu)].$$

The new spacetime variables, $\theta, \overline{\theta}$ are fermionic 2-component spinors, therefore they are doubling the number of space-time dimensions. So that we have 4 bosonic degrees of freedom (old ones) and 4 fermionic degrees - the new ones. A field which is dependent not only on x^μ but also on θ and $\overline{\theta}$ is called the superfield.

We are usually interested in only two types of superfield which are irreducible representations of SUSY algebra - the first one are chiral superfields. They can be written in a form

$$\Phi(x, \theta, \overline{\theta}) = \phi(x) + \sqrt{2}\theta^\alpha \psi_\alpha(x) + \theta^\alpha \theta^\beta \varepsilon_{\alpha\beta} F(x)$$

Field ϕ and F are normal scalar bosonic field (e.g. Higgs), ψ^α ia a spinor, like an electron. We would like to construct a supersymmetric Lagrangian from this field. Therefore, we are looking for objects made from this field which are invariant under SUSY and spacetime transformation. When we apply this on the above field example, we would find that fermionic part become bosonic and viceversa. The function F transforms as a total derivative. Because total derivatives added to the Lagrangian does not change the action, the supersymmetric Lagrangian should be constructed from these so-called F-terms.

Something similar we may do for the other irreducible representation of supersymmetric algebra: vector superfields, this means the self-conjugated fields. So that we look for its parts which are invariant under SUSY transformation or transforms as total derivative. Indeed there are some D-terms terms which transforms as total derivatives.

Now we may construct the supersymmetric Lagrangian. The basic demand is that

$$\delta_S \int \mathscr{L}(x)\mathrm{d}^4 x = \delta_S \int (\mathscr{L}_F(x) + \mathscr{L}_D(x)\mathrm{d}^4 x = 0$$

In general we use products of chiral superfields (which are again chiral superfields) and product of a chiral field and its complex conjugate is vector field. The first ones give us mass terms and the interaction terms, while the vector fiels give us kinetic terms. The detailed view of the SUSY Lagrangian is beyond the scope of this text, so reader may only refered to [7].

When we have a Lagrangian, we have to perform some spontaneous symmetry breaking. This is necessary because if there were an exact supersymmetry (this is that masses of particles and sparticles are identical), we would have seen some sparticle (supersymmetric partner of ordinary particle) by now. This is done by addition terms in Lagrangian which spoils the supersymmetry for lower energies.

The simplest supersymmetrical model is the MSSM, or Minimal supersymmetrical extension of the SM. It takes all the particles/fields from the SM, defines their superpartners and add only these terms which are necessary for the realistic model. Also, on top of supersymmetry breaking we have to do also spontanneous electroweak symmetry breaking, to obtain masses. Although supersymmetry relates some parameters of the SM, the supersymmetry breaking terms introduces some 100 new parameters. More on gauge supersymmetric theory is at [13].

One of the conservation laws we use when constructing the MSSM Lagrangian is a so-called R-parity. This means that only vertices with even numbers of sparticles are allowed. The implication of this is that the lightest supersymmetrical particle (LSP) is stable, because the vertex with incoming sparticle and outgoing ordinary particle(s) is not allowed by R-parity.

The existence of stable LSP can have far reaching consequences in cosmology. Observation showed that about 22 % of total universe energy density is composed from so-called dark matter. We cannot see it directly (therefore the name "dark"), but we can calculate its energy density from the gravitational effects. It has been proposed, that dark matter is in fact made of the lightest supersymmetrical particle(s), just like our known world is made of protons and neutrons. Also calculations are being carried out which compare the measured energy density of the dark matter and the proposed energy density of LSP. Now it seems quite probable, that if the R-parity is unbroken, the dark matter is made from LSP. However, it is still one of the open questions of the SM.

Chapter 2

ATLAS detector

Next year the LHC will be finished and will start to accelerate the beams. Its key parameters are summarized in the Table 2.1. There are four major detectors along the collider in which the pp beams can collide. Their location is shown on the Figure 2.1. These experiments are:

ATLAS (**A T**oroidal **L**HC **A**pparatu**S**) is a general purpose detector designed to exploit the full LHC potential. It is being built at Point 1 (see Fig. 2.1). The project involves collaboration of more than 1800 scientists and engineers from 34 countries. Although ATLAS main task is to search for the origin of spontaneous symmetry breaking in the electroweak sector of the SM, it is designed to measure the broadest possible range of signals. Because of unprecedented energy and collision rate of the LHC, the ATLAS will be larger and more complex than any other detector. The main lines of the ATLAS research are:

- The search for the Higgs boson or any other mechanism of the electroweak symmetry breaking
- The investigation of CP violation in B-decays
- The precise measurement of mass of heavy particles like top quark or W boson
- The search for supersymmetric particles or any other new models of physics
- The studies of compositeness of fundamental fermions

To fulfil these goals the ATLAS consists of several components which together provide as much information about the collision as possible. These subdetectors will be described later.

Table 2.1: LHC parameters

particles used	protons and heavy ions (Pb^{82+})
circumference	26.659 m
injected beam energy	450 GeV (protons)
beam energy at collision	7 TeV
magnetic field at 7 TeV	8.33 Tesla
beam luminosity	10^{34} cm^{-2}s^{-1}
integrated luminosity/year	100 fb^{-1}
protons per bunch	10^{11}
operating temperature	1.9 K
revolution frequency	11.2455 kHz
power consumption	120 MW

CMS (**C**ompact **M**uon **S**olenoid) is also a general purpose detector. The name "compact" means that it is somewhat smaller than ATLAS (about 8 times in volume), but has about twice its weight. It is being built at Point 5 (cf. Fig. 2.1) - unlike ATLAS it is being assembled on the surface and lowered to the experimental cavern afterwards. The name also signalizes that CMS is optimized for tracking muons. Its magnet will be the largest solenoid ever built, producing a magnetic field of the strength of 4 Tesla. The CMS collaboration involves about 2000 scientists and engineers from 36 countries. The scientific goals of the CMS are similar to that of ATLAS, namely

- The search for origin of the spontaneous symmetry breaking (Higgs boson)
- The search for physics beyond the SM - for example supersymmetric particles
- The study of heavy ion collisions and of the formation of the quark-gluon plasma, emulating thus the very first moments after the Big Bang

Although the construction of two similar detectors may seem as a waste of time and money, it fulfils the natural requirement on experimental physics - that any result should be independently confirmed. Also, thanks to the combined statistics from both experiments, we can reduce systematic as well as random errors.

ALICE (**A L**arge **I**on **C**ollider **E**xperiment) is a detector specially designed to study the collisions of heavy ions. Experiments in the CERN in 1990's and in the Brookhaven National Laboratory in 2000's showed that at very high temperatures the quarks are probably not confined inside hadrons but they are are rather free in a state which was called the quark-gluon plasma (QGP). It is supposed that this state of matter exists naturally inside the quasars and that it was also one of the initial stages of the Universe.

The LHC should create the quark-gluon plasma by colliding nuclei of lead with an energy of 5.5 TeV per nucleon. The QGP will be then identified thanks to the specific signatures of leaving particles - for example the production of strange particles and the suppression of the production of J/ψ mesons (made from charm and anticharm pair of quarks), because the turmoil of QGP prevents forming of heavy quark pairs.

ALICE is being constructed at Point 2 and its collaboration involves more than 1000 people from 28 countries.

LHCb (**L**arge **H**adron **C**ollider **b**eauty) is an experiment devoted to the measurement of CP violation. It is expected that it could be most clearly seen in the difference between the decay of Bd meson ($d\bar{b}$) to J/ψ ($c\bar{c}$) and K^0 ($d\bar{s}$) and the decay of anti-Bd meson to respective antiparticles. By studying the difference in the decay times, we would be able to determine the complex phase of CKM matrix [1].

This type of experiment has been already tried (among others) at the LEP, SPS or Tevatron. At present it is being tried at the b factories like BaBar or Belle. Nevertheless, none of these machines produced enough b quarks to observe such a subtle effect like CP-violation with enough significance. The LHC is able to produce much more b quarks than previous accelerators, thus hopefully making the observation of CP-violation possible.

The LHCb is located at Point 8. This experiment has nearly 900 participants from 13 countries.

The most complex of these detectors are of course the two general purpose experiments: ATLAS and CMS. They have to be sensitive to all types of particles over the very large range of momenta and energies. Also they have to be as precise as possible, because the difference between the Standard Model and the theories beyond it may be very subtle.
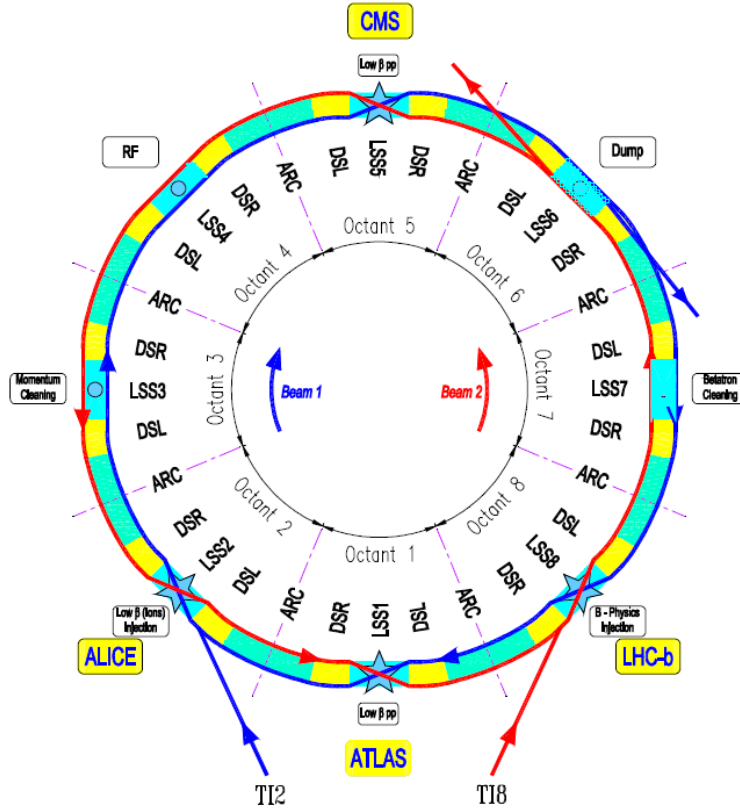
Figure 2.1: Layout of the Large Hadron Collider. Figure from [19].

Therefore these detectors are composed from various subdetectors which cooperate to fulfil above mentioned requirements. Because I am participating on the ATLAS experiment, I will focus on this detector in the following text.

The ATLAS detector is composed from the three major parts (fig. 2.2). From the center to the perimeter they are the Inner detector, the Calorimeter and the Muon chambers.

2.1   Inner Detector

The purpose of Inner detector is to provide detailed tracking information about the first part of the particle's trajectory. That means information about pseudorapidity η^1, polar angle ϕ, transverse momentum p_T and the vertices positions. This detector consists of the very precise semiconductor trackers with extremely high granularity as well as from the drift tubes with somehow less precision but a large number of hits.

The whole inner detector is set into a large solenoid, which provides field of about 2 T. This allows us to easily distinguish between the charged and neutral particles and measure their charge.
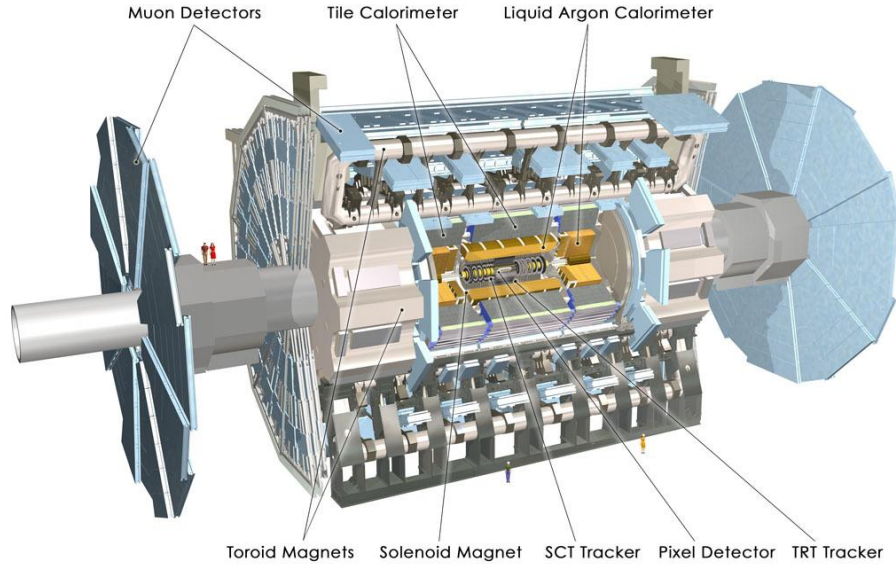
Figure 2.2: Overall view of the ATLAS detector. Figure from [18].

2.1.1 Pixel Detector

The innermost part of the Inner Detector is the Pixel detector. Its detailed view is on Figure 2.3. We can see, that it has three cylindrical layers in the "barrel" area and 3 disks in each "endcap".

The layers are labeled as B-layer (it is 5.05 cm from the beamline), Layer 1 (8.85 cm from the beamline) and Layer 2 (12.25 cm from the beamline). The barrel cylinder is 80.1 cm long. The three disks are located 49.5 cm, 58 cm and 65 cm away from the center of the detector. Their inner radius is 9 cm and outer 15 cm.

Each layer can further be divided into ladders which are essentially 13 modules with the same ϕ coordinate. They are labeled form -6 to 6, i.e. module number 0 is just around the interaction point and the modules 6 and -6 respectively are on the edges of the barrel. The numbers of staves at each layer are 22, 38 and 52 respectively.

On the disks the modules are arranged like a fan (cf. Fig. 2.3). Every disk is divided into 8 sectors with 6 modules at each of them. On both barrel and endcaps, the modules overlap to assure that the detector is hermetic with respect to outgoing particles[2].

The pixel module is shown on the Figure 2.4. It is about 6 cm long and 2 cm wide and hosts more than 46000 pixels, each of size 50×400 μm. The read out is done by 16 chips, each serving an array of 18×160 pixels. These are arranged to form a two-dimensional field, so that the pixel modules can offer extremely precise measurement of two coordinates of the track.

In the Table 2.2 there is summarized performance of the pixel detector as well as other parts of the Inner detector.

The Pixel detector is constructed to be as close to interaction point as possible and to give most precise measurements of the tracks and the vertex positions possible. The usual particle will left 3 hits in the detector, but for example cosmic muon (see chapter 4) can left much more

---

[1]Pseudorapidity is defined as

$$\eta = -\ln \operatorname{tg} \frac{\theta}{2}$$

where η is azimuthal angle ($\theta = \frac{\pi}{2}$ is vertical direction). It is a handy variable used to approximate the rapidity in case we do not know the mass and the momentum of the particle.

[2]This is not completely true. There are known to be tiny 'holes' in the overlap regions. Also, not all modules have overlap.
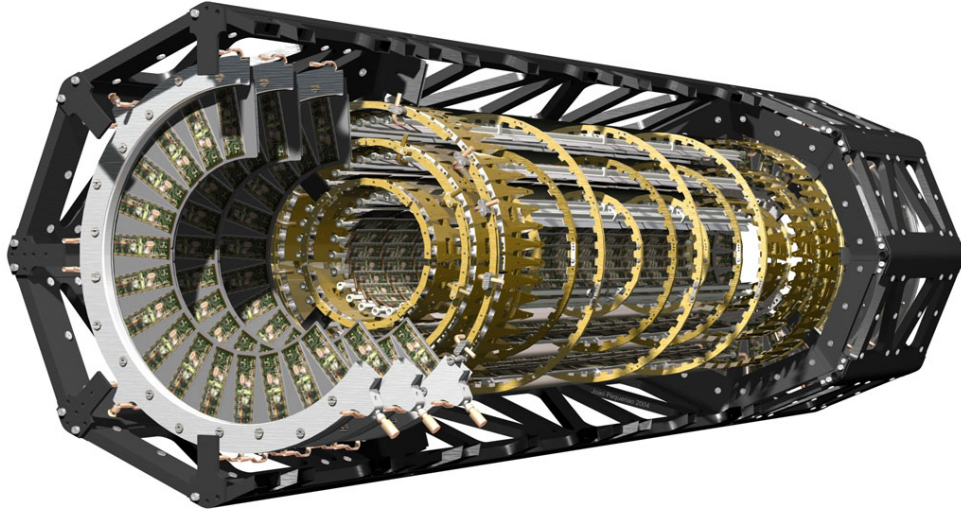
Figure 2.3: View of the inside of the Pixel detector. Three forward endcap disks are clearly visible as well as overlapping modules in the barrel layers. Figure from [18].

hits, because it can go through the detector. Also, because cosmic muons are often approaching the pixel detector from tangent, rather by perpendicular direction, it is much more probable that the cosmic muon will hit adjacent pixel modules in the same layer.

2.1.2 SCT

The Semiconductor Tracker is designed very similarly to the Pixel detector, but instead of pixels it uses the silicon strips for detection. So that the main difference is that active parts of SCT form an one-dimensional field, i.e. SCT are very precise in the ϕ direction, but less precise in the z coordinate. Look in the Table 2.2 for details.

There are 2 active layers on each SCT module so that the small difference in r coordinate of both layers allows us to measure particles's z coordinate.

2.1.3 TRT

Transition Radiation Tracker is the last (and largest) part of the Inner detector. It is built from the straw detectors, whose diameters are 4 mm and the central wire has diameter 30 μm. In the barrel, the straws are 144 cm long, in the endcap they are a bit smaller.

TRT detects the transition radiation photons which were created by passing-by highly energetic particles and so it can distinguish between the electrons and hadrons (typically pions) because each creates a different number of these photons.

Unlike semiconductor detectors like SCT od Pixel detector, the straws in TRT are relatively cheap and the particle do not lose too many energy. The TRT can give about 36 hits for the average particle.

2.2 Calorimeter

The primary purpose of each calorimeter is to measure the energy of particle. They are very dense and usually makes the particle to stop in the calorimeter and therefore deposit all its energy there as an electromagnetic or hadronic shower.
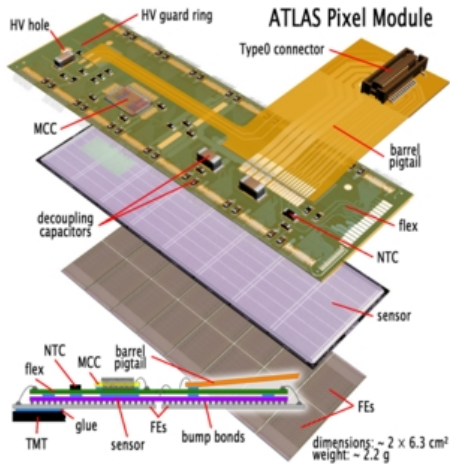
Figure 2.4: Scheme of the single pixel module. In the most bottom layer we can see the 16 readout chips. Figure from [40].
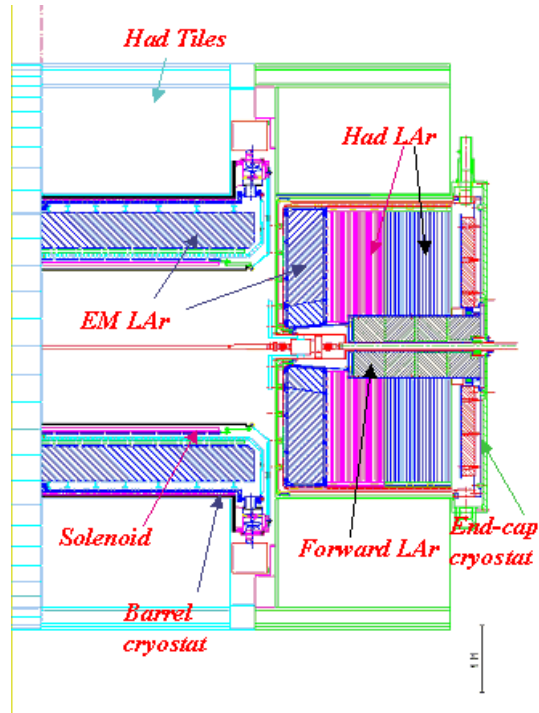
Figure 2.5: Schematic view of the ATLAS calorimetry. Both Liquid Argon and Tile calorimeters are visible. Figure from [18].

ATLAS calorimeter consists or two different parts. The first one is the Liquid Argon calorimeter. LAr Calorimeter has three parts: electromagnetic calorimeter, hadronic calorimeter and forward calorimeter. The EM calorimeter is made from accordion shaped lead electrodes which has liquid argon between them. It is both in the barrel and in the endcaps (2.5).

Hadronic LAr calorimeter is in the endcaps and uses copper plates in liquid argon to stop hadrons. Forward calorimerer is located very close to the beampipe to cover particles with large pseudorapidity. It is made from copper and tungsten.

The Tile Calorimeter makes use of steel as the absorber material and scintillating plates read out by wavelength shifting (WLS) fibres as the active medium. The calorimeter has quite high granularity - it consists of towers which have size 0.1×0.1 in $\Delta\eta$ and $\Delta\phi$. It has also very quick response which makes it ideal trigger device. The structure of ATLAS calorimetry is on figure 2.5.

Table 2.2: Inner Detector Subsystem parameters

System	Element size	Resolution	η coverage
Pixels	50×400 μm	$\sigma_{R\phi} = 14$ μm $\sigma_z = 87$ μm $\sigma_R = 87$ μm	$\pm$ 2.5
SCT	75 or 112.5 μm $\times$ 12 cm	$\sigma_{R\phi} = 15$ μm $\sigma_z = 770$ μm	$\pm$ 2.5
TRT	4 mm diameter 150 cm long	$\sigma_{R\phi} = 170$ μm	$\pm$ 2.5

2.3 Muon Chambers

The only detectable particles which may traverse through the whole ATLAS are muons. They are energetic enough not to be stopped by calorimeters and also have sufficiently long lifetime not to decay inside the detector. Therefore, there is an outer envelope of muon spectrometers which measures their momenta with high precision. This is very important, because typical trigger for hadronic collider like LHC would include the existence of at least one high-energy muon. The precise measurement of their momenta helps to reconstruct the mass of particle from which they originated - this could be for example the Higgs boson. [3]

In the barrel region ($|\eta| < 1$) there are three layers of muon chambers consisting of presice Monitored Drift Tubes (similar to the TRT from the Inner Detector) and fast Resistive Plate Chambers (RPC) used for triggering. In the endcap regions, these detectors are placed vertically, also in three layers. There are, apart from the already mentioned MDT, Thin Gas Chambers, which are also used for triggering. In the regions with high pseudorapidity (i.e. high particle flux), the MDT are replaced by Cathode Strip Chambers which are more radiation tolerant.

2.4 Magnets

The whole ATLAS is set in a very strong magnetic fields which is used to bend the tracks of charged particles. The field is generated by 2 system of magnets. The first one is the already mentioned solenoid magnet which is between the Inner Detector and the Calorimeters. It generates field of 2T.

The second system are Toroid magnets which are on the perimeter of the whole ATLAS detector, together with the muon chambers. Barrel Toroid (8 coils with air core) is designed to provide 3.9 T. The Endcap Toroid is essentially one large cryostat and should provide a field of 4.1 T.

2.5 ATLAS Trigger

When running at the full luminosity, there will be a bunch crossing every 25 ns and each crossing will bring approx. 20 of pp collisions. Not only that such a huge flux of information (about 10^9 Hz) is impossible to store and analyze, but only very few of them will be interesting, because most of them will be ordinary low energy SM processes.

In fact, the ATLAS physics programme is like looking for a needle in a haystack. To be successful in this task, ATLAS employs a three level trigger to choose the right events. Its job is to select the bunch crossing with the interesting event which is not a trivial task - for example the next crossing happens before the photons from the first one are able to reach the edge of the detector.

The level 1 trigger uses only a very limited subset of information obtained from the calorimeter and the muon chambers (RPC and TGC). But that is enough to make a choice, because in ATLAS we are interested in events with massive particles (100 GeV and more) which quite often decay into leptons. The selection is based on direction, transverse momentum and energy sums, so that L1 typically selects high p_T leptons, hadrons or jets.

L1 trigger needs about 2 μs to reach its decision and then the information is passed to the level 2 trigger. It uses full information from the detectors, but only from the regions selected by the L1 trigger - so called Regions of Interest (cf. Fig. 2.6). The L2 Trigger lowers the data flux to approx. 1 kHz.

---

[3]We know that direct exlusive decay $H \to \mu^+\mu^-$ is quite rare, but on the other hand, the muons are semi-final products of most of Higgs decays.
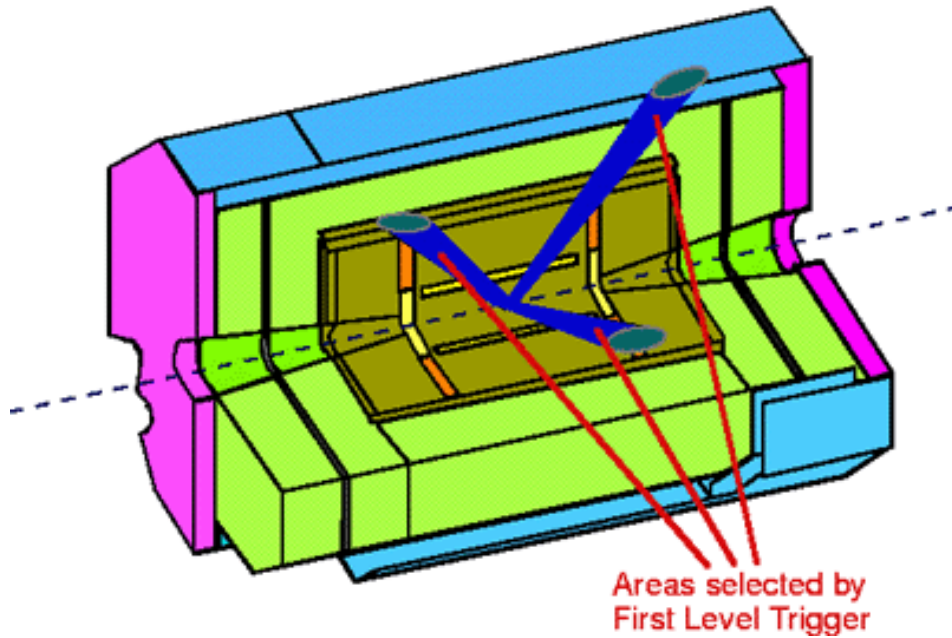
Figure 2.6: Example how the Regions of interest selected by L1 Trigger may look like. Figure from [18].

The level 3 trigger finally channels the information from the detectors to the permanent data storage. But before that it further filters the events selected by L2 trigger using all information from all detectors. At this stage rather complicated selection criteria of the offline analysis can be applied. L3 trigger also does the event building. This means it collects the pieces of information connected to one event from various detectors and put them into a single memory. The writing to the permanent data storage is done with frequency of about 100 Hz, more than million times lower than the initial information flux.

Chapter 3

ATLAS offline software

3.1 Offline Software Framework

Last chapter showed that the amount of data coming from the experiment is tremendous, impossible to handle without computers. The software which run during the data taking is called online software. Its task is to select data (trigger), store it properly (DAQ - data acquisition), control the hardware and the common infrastructure like cooling or electricity distribution(DCS - Detector Contro System), do online monitoring etc.

In contrast to that there is offline software, which could be run whenever and wherever needed. It includes various algorithms for reconstruction of tracks from the data, for analyzing and visualizing them. The software for event generation and particle simulation is also ranked among the offline software. All parts of offline software will be discussed in more detail later in this section.

Because there are hundreds or thousands of physicists willing to analyze data from ATLAS, the collaboration would be impossible if each of them will use his own algorithm, not to mention that most of them are not experts on programming.

On the other hand, if there would be just one programme (e.g. MS Atlas Analysis®), there would be no need for having different physics teams because everyone would have identical results.

Possible solution to this problem is the introduction of a software framework. This means, that there is a set of common methods and data types which are then used to construct more complex algorithms. If the pool of common tools is robust enough, everyone can build algorithms which perfectly suit her or his needs and in the same moment, this algorithm is understandable for all other members of the collaboration. Moreover, the software framework encourages the common approach and reusability of the code.

In case of the ATLAS experiment, there is an offline software framework called Athena. It is based on C++ and therefore object oriented. It encompass not only the reconstruction and analysis algorithms needed for the ATLAS data, but also all other software needed for the HEP computing. The software can be divided into 5 groups, but the distinction is not always perfectly clear.

Generators The primary task of a generator is to create an output (list of outgoing particles, their position and momenta) of some physical process if we know the initial conditions. For example we have colliding electron and positron at center of mass energy 100 GeV and we would like to know what can emerge from this reaction when we would repeat the collision a lot of times. The ideal way to do this is to use some Monte Carlo generators. Naturally, this machinery can be used also for more complex events, like hadron collisions, because the parton distribution functions are basically only other probabilistic distributions. It is

obvious that the accuracy of the generator is highly dependent on our knowledge of the underlying physical theory.

But the generators can done more than this. They can deal also with the parton showers, the hadronization and jet formation. Because we do not have an analytic theory of this, the generators usually use some data based models. Modern generators also take into account effects like underlying event (i.e. low-p_T processes).

Some generators are able to do all this tasks (like Pythia or Herwig), some of them are specialized in just one (like hadronization).

There are several generators included into Athena, most of them for the specific tasks like cosmic rays generator, but there is also an "all purpose" generator - Pythia. Although Pythia is written in FORTRAN, we can use it without knowing this language, because the Athena provides a C++ interface for her.

Simulation The input of a simulator is some physical Lorentz 4-vector describing initial state of a particle and the geometry of the event (e.g. the shape and composition of the detector). The output is a hit collection, i.e. a set of all hits (a particle coming through an active detector volume) in the various parts of the detector together with information like deposited energy, incoming direction etc.

The simulation is usually the longest part of the whole software chain from the generation of the particles to the analysis. The reason is that the simulator has to carefully propagate each particle through matter, calculate radiation losses, scattering etc.

The most widely used simulation program is Geant4, which is also incorporated into Athena. The quality of simulator is critically dependent on the quality of input data especially geometry model. It has to have granularity large enough to be realistic, but on the other hand it cannot be too much detailed, because of the computing time it would take.

Digitization The tasks of this algorithm is to take the hits vector and to assign it the response of the detector we would get if we had actually performed the experiment.

The digitization also takes into account the imperfection of detectors and finite resolution of detectors. Also, it cares for the production irregularities like the "noisy" and "dead" pixels which are included in the digitization of the Pixel detector.

As it was stated above, the output of digitization is technically identical to the output of detectors. Therefore the digitized data are ideal to test our computing system if it is able to handle the real data from ATLAS.

Also, the digitization of the generated events has another important purpose: by comparing the digitized and real data we may test the quality of our generators and simulators. Usually, also the "MC truth" (the data from generator) are included in the digitized data for reference.

Reconstruction As was mentioned earlier, the main task of the reconstruction is to take the digital signal from detector, find hits and then try to fit a track to it. There are several reconstruction algorithms and in Athena user can choose which of them would be good to use. The most used ones are xKalman, iPatRec and New Tracking.

The output of reconstruction is then similar to the output of simulation, because basically you have something like: "a particle with mass m and momentum p caused a hit in these and these places". It also tells things like charge or spin, if the detector is able to measure them. By comparing the reconstruction output with the MC truth we may measure the efficiency of the reconstruction algorithms.

Analysis The last part of the offline software chain is the physics analysis. In contrary to the reconstruction algorithms which has to be certified by ATLAS physics convenors, analysis algorithm can be written by every user. The purpose of it is to take the information from the reconstruction and guess what actually happened - for example by plotting the invariant mass of the muon pair in the $Z \rightarrow \mu\mu$ events, user will find gaussian peak, centered on the Z mass - this way a mass of the unstable particles can be measured.

Nevertheless, if it would be so easy, there would be no need for particle physicist and everything could be done by programmers. The physical insight is necessary the moment we come across something we have not seen before and therefore something completely unknown to our algorithms. In this moment, the physicist has to decide which events contain the "new physics", decide what observables is good to plot (obviously, he has to understand what they means), and of course, interprets the result.

Important part of the analysis is also the visualization of the data. This could be done essentially in two ways - first is to visualize the whole statistics in form of various histograms, cuts, fits etc. Favourite tool for this is ROOT, which will be dealt later in this chapter.

The second approach is to visualize single event, by drawing all tracks of all particles which participated in that event. This helps us to decide almost instantly whether some event was interesting or not. In case of ATLAS this job is done by Atlantis.

Atlantis is a stand-alone event display. Unlike Athena it could run on many platforms including Windows or Sun. The only thing it needs is functional Java.

If a user wants to use Atlantis to view the events, he just turns on production of so-called jiveXML files in jobOption file (see below). These are then produced during reconstruction or analysis on top of the standard output. The XML files can than be easily viewed in Atlantis. The example of an event viewed by Atlantis is on the Figure 3.1. Documentation is available at dedicated website [21].

3.2   Using Athena

Athena is a very robust framework. Apart from common data types, methods and functions, it provides central software repository for all algorithms (that means that every user can use the code of all other users, which made their code part of the Athena), and also a tool for managing all Athena software - a Configuration Management Tool (CMT).

All ATLAS offline software can be browsed via web, for example using ATLAS LXR server [22]. The code is divided into dozens of independent packages, each specialized in some particular task (for example digitization of the Pixel detector). If a user finds a package that would be of use for him, it can be "checked out" using CMT. This means that the content of the package is copied to the user's local directory. As is usual in Unix, users get only the source codes which they had to compile to obtain binaries.

To run the Athena, one needs not only the compiled source code, but also so-called jobOption files. These are python scripts which are used to choose which algorithms will be executed and when they will be executed, to feed parameters into the algorithms and also to specify the input and output.

For configuring the algorithm the jobOptions use a lot of flags - each flag activates or disables some feature of the algorithm, or sets value of some variable. Using of jobOptions allows us to run different algorithms and to steer their execution without having to recompile them. It also means, that the knowledge of the C++ is not the necessary condition to successfully run Athena. The knowledge of Python of the and set of possible flags is enough for most users.
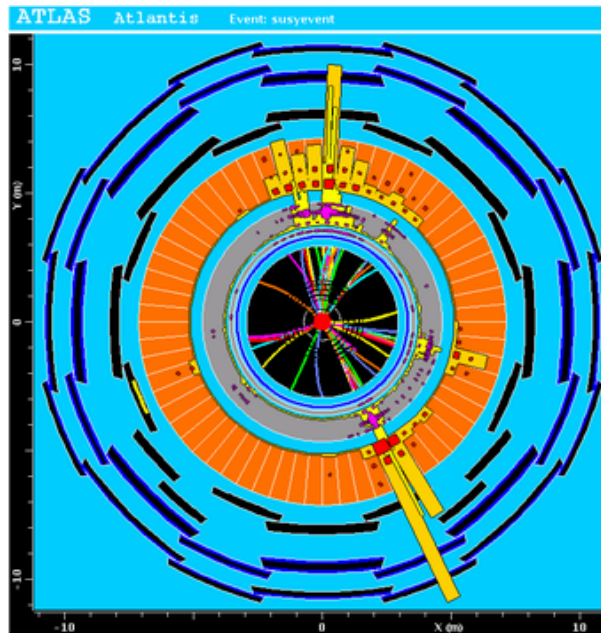
Figure 3.1: A SUSY event displayed by Atlantis event display. Figure from [21].

The Athena package is usually delivered with a set of jobOptions which can be used to perform typical tasks with the algorithm. So that by using copy and paste one can make a jobOption file according to its needs without even knowing the Python.

Athena is under continuous development, so to keep an order, the software is divided into releases. The actual release (August 2007) has number 13, but soon will come release 14. The release is basically set of software packages which was tested to be working together. This amount of testing is of course different in production releases which comes every 3-6 months and are denoted like 13.0.X. the development releases, coming every month (denoted 13.X.0) and the nightly releases, which are basically the newest code and are not tested at all.

Other consequence of the continuous development is that the documentation is still a step or more behind the actual status. The main sources of information about the Athena are ATLAS Twiki pages [23], static (or classic) ATLAS software pages [24], Doxygen documentation [25] and the hypernews [26].

ATLAS TWiki pages are based on the concept of wiki - that means that every user can write her or his experience with some problem and how to solve it. Or just describe how the user is doing her or his job. Because everybody can contribute, Twiki pages are like blackboard in a discussion room where everybody can write notes. The advantage is that nowadays Twiki covers really a lot of topics, but the disadvantage is that you can never be sure, that there are no mistakes. Also the topics are most often incomplete. Recently a campaign validating Twiki pages was launched, so that if user comes across a page with a logo "validated", he can be quite sure, that the information is useful.

Static pages covers less than Twiki, but the content is made by Athena developers, so that is more accurate than Twiki.

Doxygen is the complete code documentation, however is mostly very technical. User can quickly found here how is some method or data type defined, but if he does not know C++, he would not be any wiser after using it.

Probably the most useful source of information and help is the hypernews - a collection of

web based e-mail conferences on some topic (e.g. alignment, pixel offline software, etc.)

3.3 ROOT

A paragraph about physics analysis briefly mentioned ROOT as one of the analysis tools. Similar to Athena, ROOT is also C++ based software framework, although not so robust. Because ROOT is specialized in high-energy physics, it provides classes like Lorentz Vector or Histogram, etc. This can be used in constructing ROOT algorithms.

There are basically two ways of using ROOT. The first one is interactive mode - a user writes the C++ statements on the command line and they are executed by ROOT interpreter. The second way is to write some script, store it to the file and then execute it. The script can be also compiled which speeds up the calculation approx. ten times.

ROOT is able to do many things, but the most used feature is plotting histograms - it is able to do many different types of histograms which users can simply edit via ROOT graphical user interface.

Apart from histograms the ROOT is able to do a lot of mathematical tasks like infinitesimal calculus or linear algebra. It can cooperate with OpenGL, so that it is also used in making fancy 3D models of the detectors and other devices. ROOT can also draw the Feynman diagrams.

ROOT stores its output to its own filetype. Typical suffix is .root. This format is very economical in means of ratio between stored information and the actual file size. Therefore it is used also by Athena as a typical output or input.

Although ROOT starts with a command line interface, it is possible to turn on graphical user interface - user just has to create an instance of the class TBrowser. This opens a browser, where one can open a root file for editing.

ROOT is very popular in HEP community and is used not only by ATLAS collaboration, but rather by most of experimental particle physicists and even by people from other professions who need a program for data analysis and visualization.

The documentation, examples and installation guides for ROOT can be found on its web site [27].

Chapter 4

Studies of Cosmic Rays in the ATLAS Cavern

4.1 Introduction

ATLAS has already been being build for several years and now the construction has reached its final phase. The various subsystems are being lowered down to the cavern and assembled to the final shape. The first active detectors (calorimeters) were put in the cavern in March 2004. Now, almost all detectors are on their places but still there is a lot of work to do - especially cooling and cabling, so that ATLAS will not be ready for data taking before November 2007.

Nevertheless, the collider will be finished even later (the first beams should be available at May 2008), so that there will be large period when ATLAS will have no particles from collisions to detect.

However, as soon as the detector will be turned on, we will have data from the cosmic rays. And, as was written above, for the long time it will be the only data available, because even after the collider will start running it will take some time until there will be the 7 TeV collisions.

The whole spectrum of early LHC physics was described in the ATLAS note [28]. It was written several years ago, so the schedule is a bit out-of-date, but the physics description is still valid. For an up-to-date LHC schedule see [29].

Although in the first years of high-energy physics the cosmic rays were used as a source of new particles and were subject of intensive studies, now the cosmic rays are known so well that they can be used the other way round - to probe our detector. This was done for pixel endcaps last year and the results told us a lot about the detector systematics. The ATLAS note [30] summarizes the results of this study.

The idea now is to do the same for the whole pixel detector when the ATLAS will be turned on. There is, however, a significant difference: the endcaps were tested on the surface while this time the detector will be properly installed in the center of ATLAS, several dozens meters below ground (See Figure 4.1).

This means that the rate of cosmic muons in the pixel detector down in the cavern would be much lower than they had for the endcaps study [30]. How much lower? The flux of cosmic muons on the see level is well known and is ≈ 1 cm^{-2}min^{-1}. The precise distribution as a function of incoming angle and energy could be found in [31] or in the [32].

The flux in the cavern was estimated from the simulation by Geant3 and subsequently it was measured in 2003 by muon telescopes. The complete results are in [28]. The essence of the result from their simulation is in the Table 4.1. We can see that only about 0.05% of surface muons eventually enter the cavern and from these also only 1 in 5000 goes through the Pixel detector, resulting in rate of slightly less than 1 Hz. The Figure 4.2 shows the good agreement
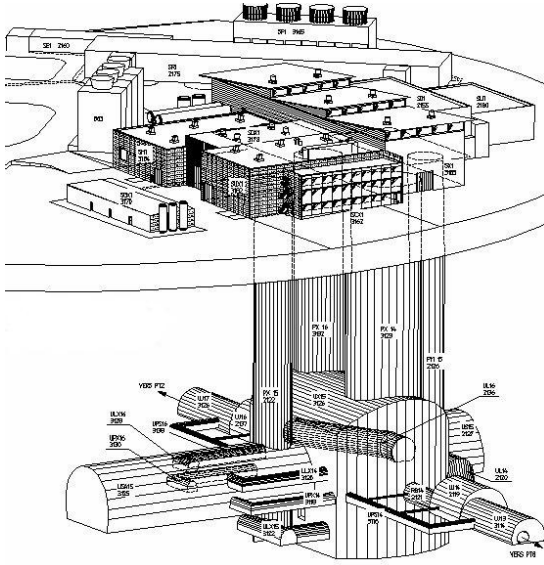
Figure 4.1: Schematic view of the ATLAS experimental cavern, access shafts and the surface buildings. Figure from [18].
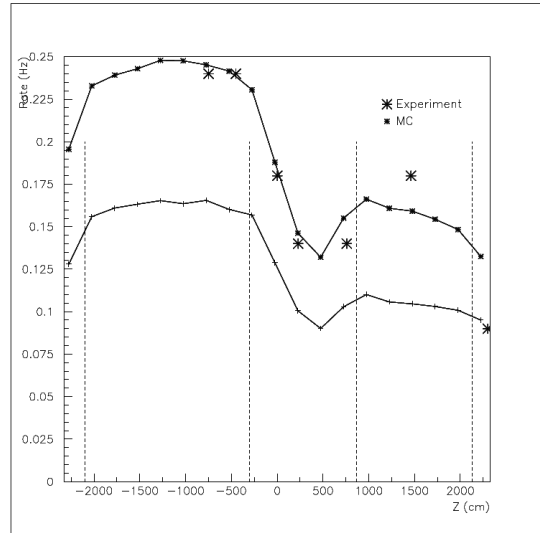
Figure 4.2: Comparison of MC simulations and measurements of cosmic muon flux in the ATLAS cavern. Upper curve corresponds to flux predicted along the central axis, the lower to the cavern wall. Dashed vertical lines symbolize the position of access shafts. Figure from [28].

Table 4.1: Results from simulation done in [28]

surface rate	$3.0 \times 10^{-3}/(\text{cm}^2\text{s})$
number generated	19×10^9
real time	1747 s
Entry cavern rate	4.9 kHz
≥ 1 hit rate	3.4 kHz
≥ 1 Pixel hit rate	0.7 Hz

between simulation and the measured flux. The question now is what can be done with an hour, two, three... etc. of the experimental data, if anything.

4.2 Cosmic Muons Simulation

To find the answer on the previous question more than just a measurement of muon rates in empty cavern is needed. We have to do the simulation to discover the effects of the cosmic rays on the detector. Of course, we would not know the *exact* effect of cosmics from simulation, but it will give us a hint on what to expect and the comparing with data also test the quality of our simulation algorithms. In fact cosmic run will be the one of the first ATLAS experimental predictions to be confronted with the data. If the results from simulation agree with the experiment we can have more confidence to detector, the simulation algorithm and the ATLAS geometry model it uses.

The code for the simulation have in principle two parts: first is cosmic muon generator and

the second is the simulator of particles in the ground, in the ATLAS cavern and of course inside the detector.

4.2.1 Cosmic Muon Generator

Twenty years ago Alois Putzer wrote a FORTRAN program to generate cosmic muons. It was based on fits to experimental data from ALEPH. The 2003 survey [28] showed that for ATLAS cavern his program was actually more precise than the PDG approximation formula. Therefore the Athena framework uses Putzer's algorithm for generating cosmic muons.

The package to generate cosmic muons is stored among other Monte Carlo generators, the full path to the package is `Generators/CosmicGenerator`. This package contains two algorithms: `CosmicGenerator.cxx` and `CosmicGun.cxx`. The first one is the master algorithm, which collects all external parameters and calls, when needed, the executive algorithm `CosmicGun.cxx` which creates a cosmic muon using Alois Putzer algorithm and the external parameters passed down by the master algorithm `CosmicGenerator.cxx`.

The input parameters for the Monte Carlo generator are:

- the spatial volume in which the muons will be generated

- maximal and minimal energy of the muons

- cosinus of the minimal allowed azimuthal angle (the value $\cos\theta = 0$ means that all downwards heading incoming angles are allowed)

Given these parameters the `CosmicGun.cxx` generates a muon (this means 4-vector with muon rest mass) according to this boundary conditions and the Alois Putzer's distribution functions. However, the master algorithm `CosmicGenerator.cxx` can do selection of the muons at the generator level. The parameters for selection are:

- position of the ATLAS interaction point

- the radius of the optimizing sphere: this means that only these muons which are heading to the sphere of given radius around the interaction point are selected for further processing

The older versions of this algorithnm contained a disturbing bug when the sign of the vertical axis was flipped, i.e. the generated (and selected) muons were heading upwards. This was fixed since the version `CosmicGenerator-00-00-24` which was also used as a source of cosmic muons.

4.2.2 Geant4 simulation

The output of the Cosmic Genenerator is a 4-vector pointing to designated distance from the center of the ATLAS. It represents cosmic muon's 4-momentum and is used as an input for the simulation.

That is done by Geant4, but still within the Athena framework. The Athena code for simulation is contained in the package `Simulation/G4Atlas` which serves as an interface between Athena and Geant. It contains several sub-packages and the master algorithm is stored in the `G4AtlasApps`. This package can simulate whole ATLAS detector together with the cavern and the overlying ground.

In the `share` directory, there is a large choice of various JobOptions, depending on what the user would like to simulate. The whole documentation for this package is accessible online at [33].

The parameters for simulation are chosen by flags. They can be divided into several groups. Detector flags are used for turning on and off various subdetectors as well as MC truth and

Level1 trigger. The Common flags are used to define the input and output files as well as other general properties like number of events to be processed. The third large group are the Simulation flags - unlike the previous two groups, they are specific to this package and are used to choose the version of ATLAS geometry or the sources of particles for simulation.

There are several versions of ATLAS geometry which are continuously updated as a new data from survey are coming. In general there are versions called "ideal" or "nominal" geometry and several versions of misaligned geometry. There are different versions of misaligned geometries depending on what level of misalignment you want to study. The current versions of ATLAS geometry are labeled in this way: ATLAS-CSC-xx-yy-zz, where the first pair labels the versions of ideal geometry and the second labels version misalignment w.r.t. ideal geometry. Full documentation for them is available on Twiki.

There are also geometries which take into account the cavern and overburden, which is extremely important in cosmics simulation. Also here one may choose from several different versions - ideal, misaligned and with or without magnetic field.

Flag `KinematicsMode` selects the source of particles. The first possibility is the external file with the generated events. The second is internal simple particle generator. There user can choose where the particle will be generated, its type (e.g. electron) and its initial 4-momentum. With the exception of the particle type, all properties could be set to be randomly generated according to given range and statistical distribution (e.g. flat or gaussian). The last type of particle source is one of the MC generators contained in the Athena `Generators` package.

One of the JobOption files is dedicated to the simulation of the cosmic muons - it is the `jobOptions.G4Cosmic.py`. This means, that the default geometry setting contains also the cavern and especially the 50 m of overburden above it. It also means that it uses the particles generated by `Generators/CosmicGenerator` as an input. The parameters for the generator which were mentioned in the previous section are set in other jobOptions file: `CosmicGenerator.py`. The standard output of this algorithm is a root file with a hits collection.

4.2.3 Determining the Cosmic Muons Rate through Pixel Detector

Our first aim was to find how often some cosmic muons hits the Pixel detector. However, the default simulation setting was not appropriate for this task. Because only a simple piece of information was needed, we chose to modify the simulation algorithm instead of analyzing the very complex hits collection.

Athena contains a package which is intended just for this task - it is called `G4UserActions` and allows user to modify what is done at the beginning and end of simulation (`BeginOfRunAction` and `EndOfRunAction`), what is done at the beginning and end of each event (`BeginOfEventAction` and `EndOfEventAction`) and finally, what should be done at each step (`G4SteppingAction`), because the simulation is made from discrete points rather than continuous track.

Having this tool at hand it was not difficult to define user actions that do the job. The principle of our algorithm is quite simple. At each step of the simulation it asks for the name of the volume it is in. If it is in active volume of Pixel detector, it also inquires about the energy of the particle and checks whether it is bigger than 100 MeV[1], about its momentum, about the hit positions, position of the primary vertex and particle's initial momentum. All these variables are recorded in the form of a text file. The layer, module and ladder number of the device(s) the muon passed through is recorded as well.

There are two types of output. One, where all the hits in the pixel detector are recorded and one where there is recorded only the first hit to keep track of the number of cosmic muons

---

[1]It is rather arbitrary choice, its main purpose was to rule out the particles which would not be detected anyway

which hit the detector.

Besides that, the stepping action also records data about muons which hit the floor of the ATLAS cavern, thus creating a "muongram" of the ATLAS.

The other actions (`BeginOfRunAction`, `EndOfRunAction`...) mainly serve as a service and support for the stepping action: they declare the variables, open and close the output files and make overall sums like total number of hits, number of hits in each layer etc.

Having modified the simulation according to our needs, the only thing which could be configured was the cosmic muons generator. As was mentioned earlier, the parameters are set by the python script, but it was not immediately clear how to choose the parameters so that the output of simulation is realistic enough and on the other hand, it could be calculated in the reasonable time.

The most realistic setting would of course be if the volume where the muons originates would be taken as infinite and if all muons were simulated. But, as computing resources and time are limited, a choice was made that at first the muons should be generated in a surface 600 m × 600 m over the ATLAS cavern[2]. There is no need for the third dimension, as the muons will have to pass through this surface anyway. The 600 m × 600 m square is however not on the ground but rather around 20 m above it, so that the simulation takes into account also the effect of surface structures.

Could this surface be made smaller? The Figure 4.3 shows that most of the hits are concentrated in the central region. However, there is still significant portion of muons coming from the bigger distance and carrying relatively large amount of energy. Therefore, by decreasing the surface too much, we would lose important information about highly energetic muons with high pseudorapidity η.

Nevertheless, we can see that there was only one hit out of 152 outside the square 400 m × 400 m. So that decreasing surface to that value would speed up the calculation approx. twice (as the surface will be less than half big), while losing about one per cent of information - this value is comparable to the discrepancy between our cosmic generator and the measured values of the cosmic muon flux [28]. So that the other samples of the simulation were done using the 400 m × 400 m surface, unless stated otherwise. The distribution of primary vertices for this setting is on Figure 4.4.

Second important parameter is the size of the optimizing sphere. This setting is even more problematic as there are two opposing effects. If we for the moment concentrate only on the computing time we will find that with decreasing radius of the sphere the algorithm has to simulate less muons which do not give any hit in the Pixel detector. However, it spends much more time in the generating stage as there is lesser probability of generating muon pointing to the smaller sphere.

On the other side, when we increase the optimizing sphere, the generation is faster as more muons are accepted, but now the simulation takes longer as we then simulate a lot of muons which miss the Pixel detector.

Another problem with the sphere comes from the physical behaviour of the cosmic muons. It is obvious that from the muons pointing towards the center of ATLAS some deflect and do not enter the sphere where they were originally heading. This is not a real problem, it only means that the simulation will be longer. The possible bigger problem is the number of muons not pointing towards ATLAS initially but eventually scattered to hit the Pixel detector. It is not easy to actually find this muons and with the present algorithm their number could be only estimated.

The Figures 4.5 and 4.6 shows the relation between the initial pseudorapidity and the pseudorapidity when hitting the Pixel detector and between the initial polar angle and the polar angle

---

[2]A choice of larger surface is not possible because it will be larger than current ATLAS geometric model, so that the attempt to simulate muon outside this model will cause program crash.
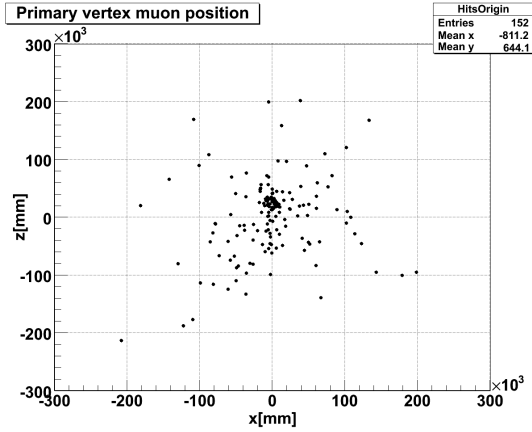
Figure 4.3: The position of the primary vertices of the cosmic muons eventually hitting the detector. View of the surface from above. Beamline is going in vertical direction.
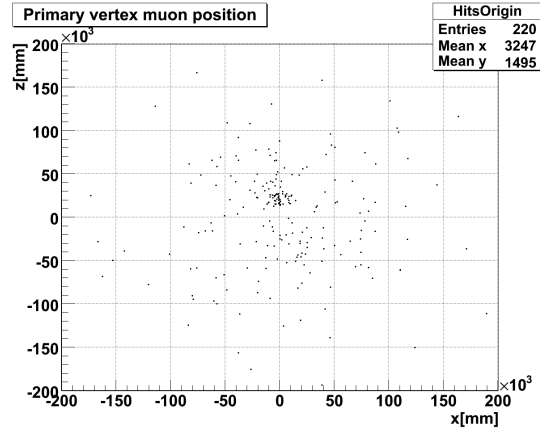
Figure 4.4: The position of the primary vertices of the cosmic muons eventually hitting the detector, generated on a 2.25 times smaller surface. View from above. Beamline in vertical direction.
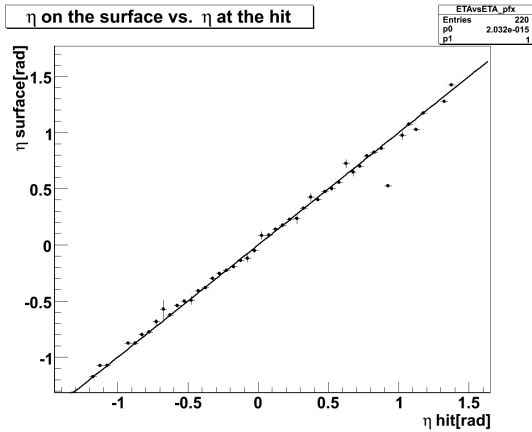
Figure 4.5: Initial value of the pseudorapidity plotted against the final value of pseudorapidity. Solid line is linear fit. From fitting parameters (in the upper right Table) reader can see, that $\eta_{\text{final}} = \eta_{\text{initial}}$, i.e. the scattering for the muons hitting Pixel detector is minimal.
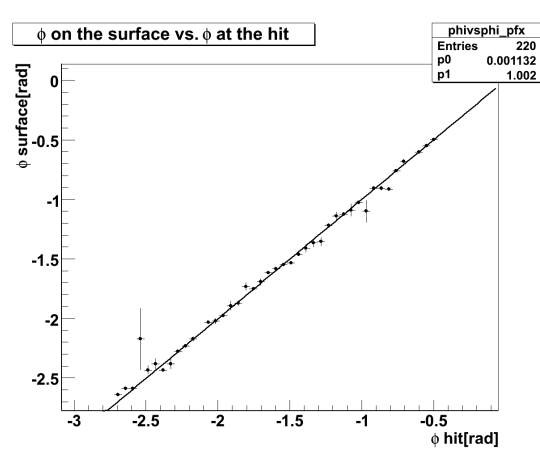
Figure 4.6: Initial value of the polar angle plotted against the final value of polar angle. Solid line is linear fit. Its parameters are in the upper tight Table. Note that vertical direction is $-\pi/2$. The scattering in ϕ direction is also minimal.

Table 4.2: Rate of the cosmic muons determined from the simulation by Geant4

Muons generated	Muons accepted	≥ 1 Pixel hit	Real time	Rate
6 907 433 412	11 575 728	220	259.6 s	0.85 Hz

when hitting the pixel detector. Both have been linearly fitted. We can see that with the exception of small angles (corresponding to shafts), the fit is almost perfect identity.

That means, that if muon is energetic enough to reach the Pixel detector, it is very improbable, that it will be scattered by some large angle out of initial direction. Therefore the muons pointing outside the optimizing sphere and able to reach the pixel detector will almost never hit the Pixel detector. So that relatively small sphere can be safely used as a generator filter. Our choice was sphere with radius 10 m (which is still much larger than the Pixel detector). Technically speaking it could have been smaller, but then, as already said, the the event generation would require unreasonable amount of computing time.

4.2.4 Results from the simulation

The first result we can deduce from the simulation data is the cosmic muons rate. The output of the program is the total number of generated muons, how many of them passed the selection criterion of pointing towards the sphere (this rules out $\backsim 99.9$ % of all muons) and how many of them enter the Pixel detector sensitive area.

To determine the rate of cosmic muons we also needed the size of flux of cosmic muons - our generator uses value 133.5 muons per second and m^{-2}. The results for rate of cosmic muons are in Table 4.2. This results are in good agreement with [28].

Now, that we know that will have at least some muons (with a week of cosmic run that would mean hundreds of thousands hits), it is good to look for their properties. The Figure 4.7 shows the energy of muons entering tracker - we can see that the distribution is steeply falling with rising energy and that the most likely are these with the energy below 1 GeV. These are the muons coming through the shafts. Also other peak is visible at about 12 GeV - this is for the muons which had to pass the overburden.

A bit different is the distribution of the initial energy for the same muons. It is on the Figure 4.8 where we can see that there are in fact two distributions - one that peaks at low energies and then it falls and the other which has peak at about 50 GeV. The first one corresponds to low energy muons coming mostly through the access shafts, while the latter distribution are muons coming with higher pseudorapidity and spending most time in the ground.

To investigate the region of low energies, a special sample, denoted as *spec1*, was produced. Basically, it focused on the muons coming through the shafts, so that the generating surface was only 60 m × 60 m and the radius of optimizing sphere was 5 m.

Indeed, if we look on the result from the special sample on Figures 4.9 and 4.10 we can see that now we have mostly low energetic muons hitting the Pixel detector, and the peak at 12 GeV for the high-energetic muons is practically invisible.

For the initial energies (fig. 4.10), we can see peak at about 6 GeV, meaning that even if the muons are coming through the shaft they still need some energy to pass through the calorimeters. The remnants of 50 GeV peak for the high-energetic muons is also visible.

This means that the simulation could be made more effective if it will be split into two - one concentrated on low energy muons, with small generating surface and low energy cut and one for higher energy muons - with larger surface and higher energy cut.

Other interesting property of the incoming cosmic muons is their direction. Figures 4.11
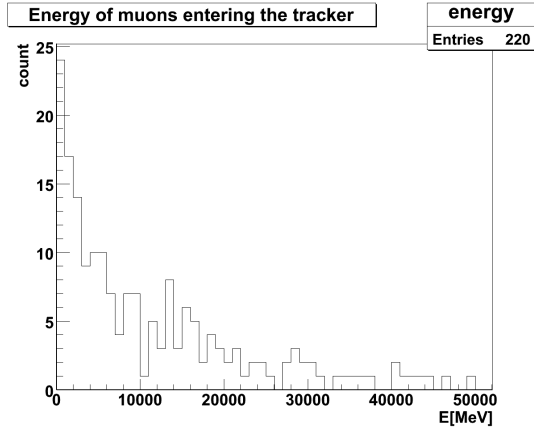
Figure 4.7: Distribution of the energy of the muons hitting the Pixel detector. Size of bin is 1 GeV
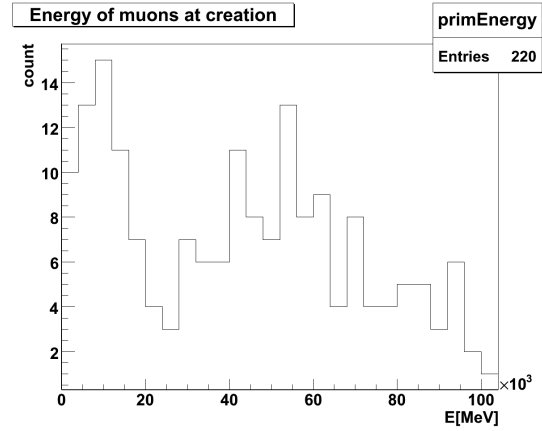
Figure 4.8: Distribution of the initial energy of the cosmic muons hitting the Pixel detector. Size of bin is 4 GeV.
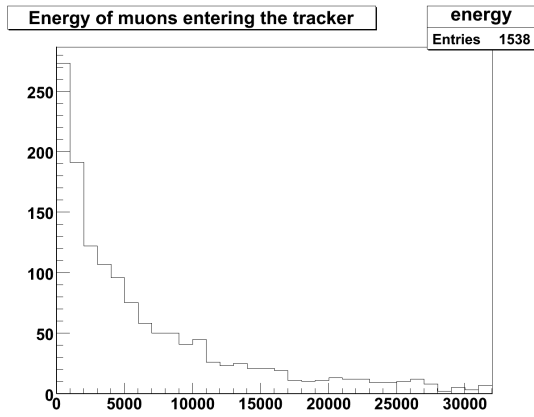
Figure 4.9: Distribution of the energy of the muons hitting the Pixel detector for the *spec1* sample as defined in the text. Size of bin is 1 GeV
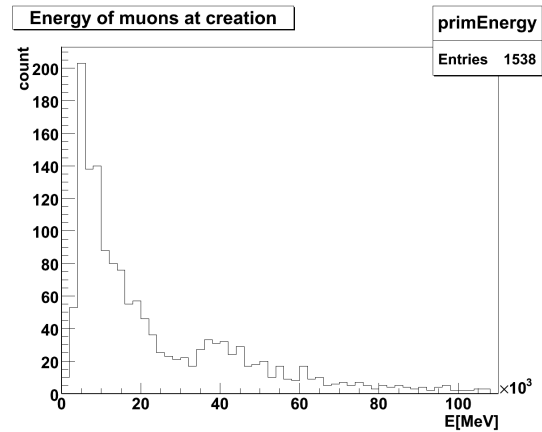
Figure 4.10: Distribution of the initial energy of the cosmic muons hitting the Pixel detector for the *spec1* sample as defined in the text. Size of bin is 4 GeV.
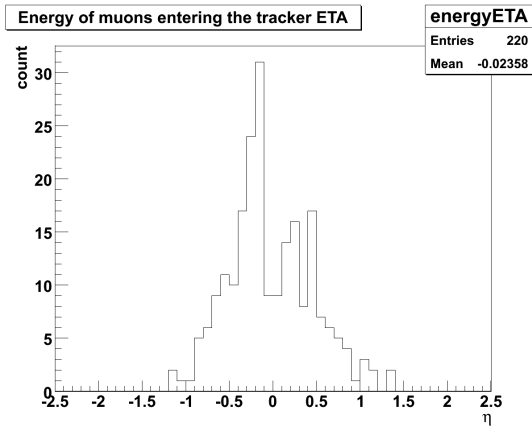
Figure 4.11: Pseudorapidity distribution of the muons hitting the Pixel detector. Note the asymmetry caused by the shafts
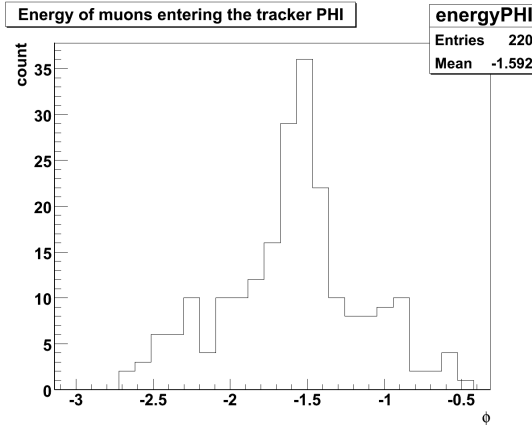
Figure 4.12: Polar angle distribution of the muons hitting the Pixel detector. Vertical direction is $-\pi/2$.
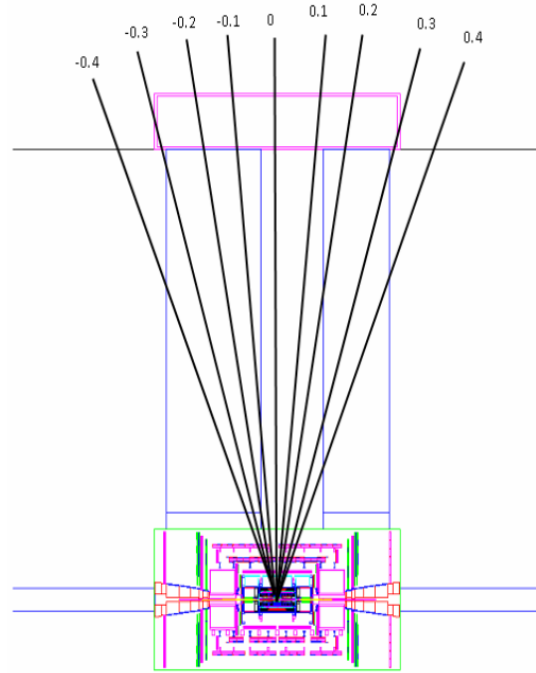
Figure 4.13: Cross section of the ATLAS cavern and the access shafts, together with the pseudorapidity regions. Figure from [34]

and 4.12 shows their pseudorapidity and polar angle distribution. We can see that their polar angle is more or less symmetric around the direction to the top ($\phi = -\pi/2$) and the distribution resembles $1/\cos^2\phi$.

Much more interesting is the η distribution. It has peak between $\eta = -0.1$ and $\eta = -0.4$, which corresponds to the main shaft - cf. Figures 4.13 and 4.1. Notice also the smaller peak at about $\eta = 0.5$ which corresponds to the second (smaller) shaft.

After the basic facts about the cosmic muon rates and distribution were found, we can look to the data in more detail to figure out, whether these hits would be good enough for reconstructing of tracks. Figure 4.14 shows the number of hits for the muons which entered the pixel barrel. We can see that mostly we have as least three hits, so that the reconstruction seems possible for most of the cosmic muons.

However, for the disks the situation is more severe. Figure 4.15 shows for endcaps the same information as Fig. 4.14 shows for barrels. Fortunately when using other parts of ID we should have enough hits to do a reconstruction, so that we will be able to use endcaps in the cosmic runs as well.

The Figure 4.16 shows the distribution of hits in the pixel detector as a function of their
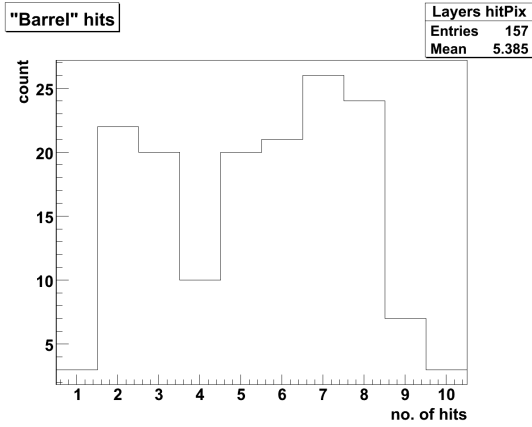
Figure 4.14: Number of hits in the Pixel detector for the muons which enter Pixel barrel.
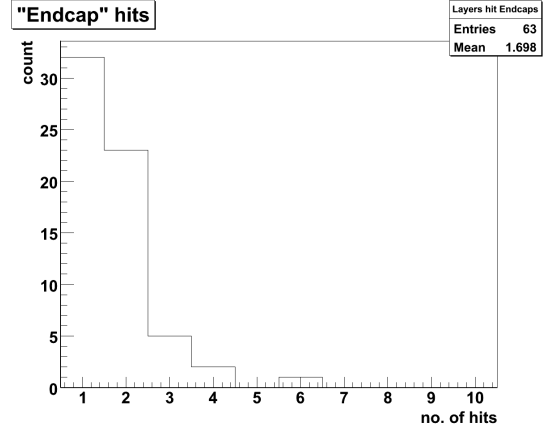
Figure 4.15: Number of hits in the Pixel detector for the muons which enter one of the Pixel endcaps.
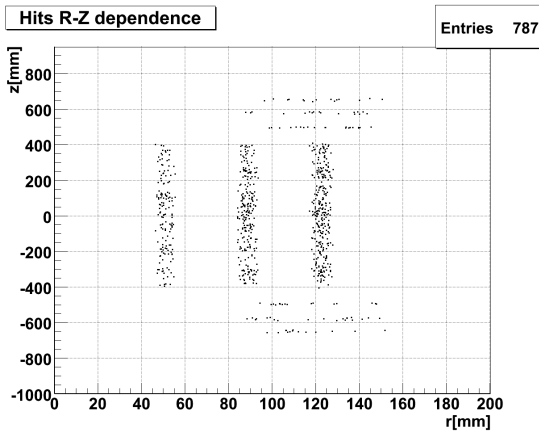
Figure 4.16: Distance from the centre and the z coordinate of the all hits in the Pixel detector. Numbers of hits in the layers are (from the centre to the edge) 149, 240 and 295.
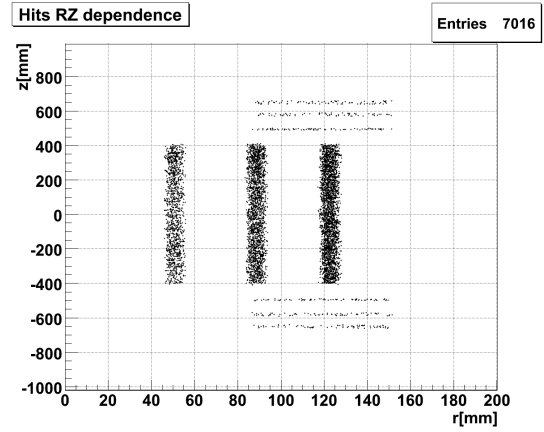
Figure 4.17: Distance from the centre and the z coordinate of the all hits in the Pixel detector. Data from the *spec1* sample. Numbers of hits in the layers are 1293, 2219 and 3053 respectively.

Table 4.3: Rate of the cosmic muons determined from the simulation by Geant4 for the *spec1* sample

Muons generated	Muons accepted	≥ 1 Pixel hit	Real time	Rate
1 950 885 440	8 407 448	1538	4060 s	0.38 Hz

distance from the beamline r and their z coordinate. We can see that the hits are more or less uniformly distributed in all layers. The low statistics however does not allow us to see all of the disks. This is changed when we look for the same picture obtained by the *spec1* sample (fig. 4.16). Here we can see all the structures of the Pixel detector clearly.

This means that we would be able to test the whole pixel detector with the cosmic rays. The question now is how long would it take to acquire such an amount of data which is shown on the Figure 4.17. The data in this Figure come from the *spec1* sample The real duration of this sample would be around 1.2 h, see Table 4.3 for the rate of muons from this special sample.

In reality we would have in the same time more hits because the special sample ignored the more energetic muons coming from high angles - you can see that rate is approximately one half of the "full" rate.

Apart from hits in the pixel detector our algorithm also stores the hits on the floor of the ATLAS cavern. This can give us some idea about the overall distribution of cosmics in the ATLAS cavern. To cover the whole cavern, a new sample was produced: the generating surface was 400 m × 400 m as before, but the optimizing sphere was somehow enlarged: its radius was set to 40 m.

The Figure 4.18 shows the density of cosmic muon hits on the floor. It is view from above, the beamline is going from top to the bottom. The shape of the cavern 4.1 is clearly visible and we can also see the effect of both shafts. The latter is even more visible on the Figure 4.19, which shows the hits only of these muons which are (nearly) nearly vertical in their initial state.

Very instructive is to compare bare hits density which is on the figures 4.18 and 4.19 with the same data weighted by the energy on Fig. 4.20. While the first Figure had clear peaks just under the shafts, the latter is somehow smeared, meaning that although the areas below the caverns have most hits, they are not most energetic.

This is even more visible on the Figure 4.21, which shows the average energy per muon. We can see that the areas below caverns are flooded with low energy muons, while the area between them has the most energetic hits. The question now is, what is the consequence for the pixel detector.

On Figures 4.22 and 4.23 we can see the density of hits in the pixel detector for both standard and *spec1* sample. Although the statistics for the first Figure are quite low we can see, that no side of the detector is preferred, i.e. the density is independent on z, and depends only on r. This confirms also Fig. 4.23.

The Figure 4.24 on the other hand shows the average energy per hit. Again no clear structure, the energy distribution is homogenous in the first approximation. It seems that there are high-energetic hits on the edges of the layers from the high-η cosmic muons, but the statistics is too low to tell this for sure.

The same holds also for the *spec1* sample 4.25. The energy distribution is practically uniform, exception is several high energy muons, depicted as a red areas on the Figure 4.25.
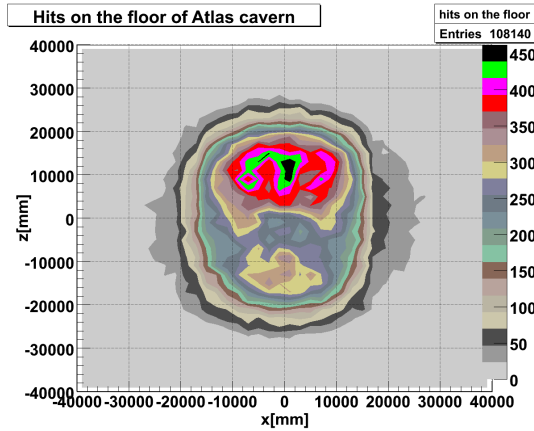
Figure 4.18: Cosmic muon density on the floor of the ATLAS cavern as viewed from above. Different colours represent different densities, see palette.
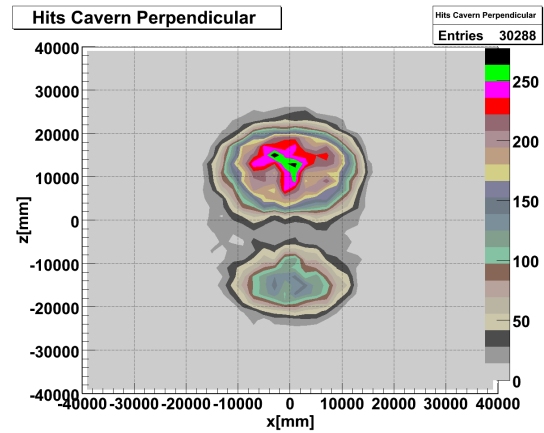
Figure 4.19: Density of cosmic muons on the floor using filter on vertical muons.
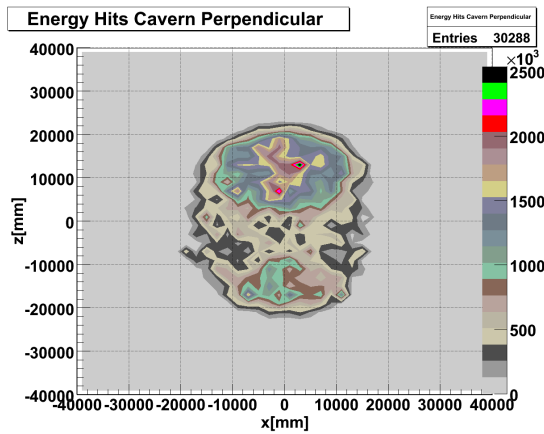
Figure 4.20: Density of the vertical muons as on Figure 4.19, weighed by their energy in MeV.
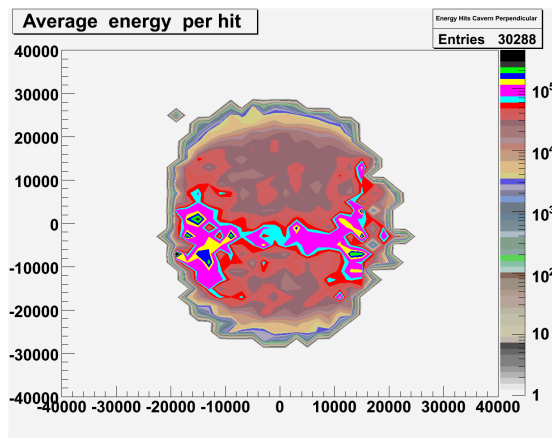
Figure 4.21: Average energy of a muons hitting some particular spot on the floor. Notice that the most energetic particles make hits outside the access shafts, while the area below the shafts is dominated by low energy muons. The energy scale is in MeV.
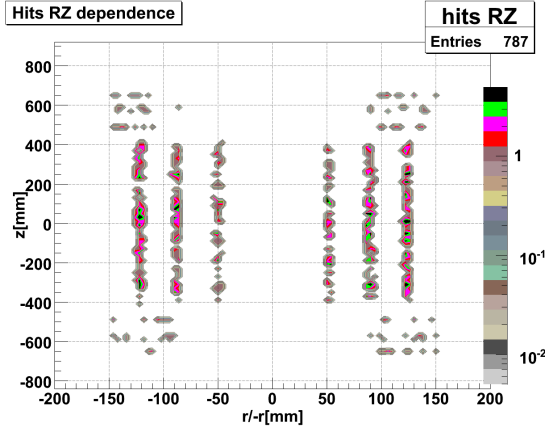
Figure 4.22: Density of a cosmic muon hits in the Pixel detector above ($r > 0$) and below the beamline ($-r > 0$. Colour palette is used to expressed different density. Logarithmic scale for density is used.
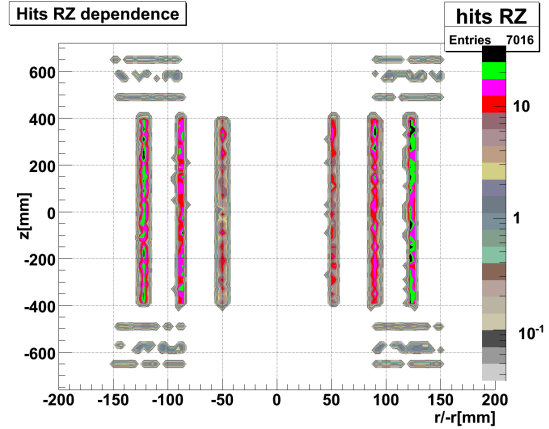
Figure 4.23: Density of cosmic muons in the Pixel detector above and below the beamline. Colour palette is the same as on Fig. 4.22. Data from *spec1* sample.
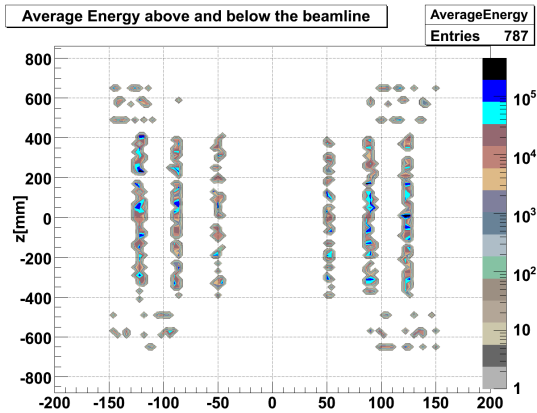
Figure 4.24: Average energy of the cosmic muons hitting Pixel detector in the various places. Energetic scale is logarithmic and in MeV.
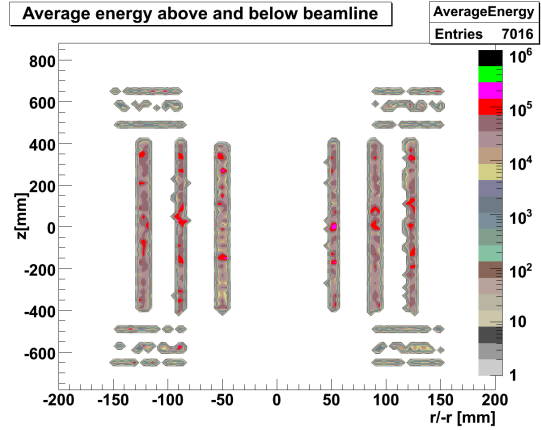
Figure 4.25: Average energy of the cosmic muons hitting Pixel detector in the various places. Energetic scale is logarithmic and in MeV. Data from *spec1* sample

4.2.5 Cosmic trigger

ATLAS was built as a general purpose detector, primarily for detecting particles originating from pp collisions. Therefore it is not optimized for the measurement of cosmic muons (indeed, it is situated so deep to have as few cosmic hits as possible). Nevertheless previous section showed that even the innermost part of the detector will have quite a lot of cosmic hits. So how can one trigger cosmic muons on ATLAS?

ATLAS trigger was designed for a high energy particles originating from collisions of proton bunches every 25 ns. Cosmic muons will, on the other hand, come from the opposite direction and in much lower rate. This means that the standard ATLAS trigger is useless for this task. So that something else will have to be used.

For the first level trigger we can use muon chambers and/or calorimeter. If we want to trigger cosmics for pixel detector, the muon chambers will not be much of use for several reasons. The main reason is that they are quite slow. The other reason is that they are constructed as a "last" detectors - usually muons are the only particles which are able to come to the muon chambers from inside the ATLAS. The logic is that every hit in muon chamber is a (high energy) muon, so that something interesting must have happened during the collision.

But from the point of view of cosmic muon, the muon chamber is the first detector which they meet. And also while almost cosmic muons hitting the pixel detector hit also the muon chambers, only a few per cent of muons hitting muon chambers hit the pixel detector. This could be improved by demanding the hits in the opposing hemisphere (i.e. the ϕ coordinate differ by π and η has different sign), so that the line connecting this two hits would go near the center of detector. However, muon chambers have too low granularity and too big distance from the center to be efficiently used for such a purpose.

What about the calorimeter, the second device for L1 Trigger? The study based on the simulation [34] showed, that triggering cosmic muons by tile calorimeter is both possible and effective. Figure 4.26 shows how would the "ideal" cosmic event look like - hitting two towers which are in opposite positions - also called "back to back" hit. Because of high granularity, this trigger ensures, that the muon is going next to the center of detector, i.e. through the pixel detector.

The tile calorimeter is divided into towers, each having size of 0.1×0.1 in $\Delta\eta \times \Delta\phi$ space. This is the smallest value. Other possible values come from grouping this tower "units", i.e. we have 0.2×0.2 and 0.4×0.4 towers. This is why the study [34] concentrated on effects of various tower sizes and the energy cuts on the trigger efficiency.

It is quite obvious that with lower energy cut and bigger tower size we would get higher event rate, but there are other effects which should be taken into account. If we are interested in the pixel detector, the tower should be as small as possible, to assure hit in the pixels. The diameter of pixel detector is roughly 60 times smaller than the inner perimeter of the tile calorimeter. And this perimeter is divided into 63 towers with the dimensions of 0.1×0.1. That means, that if we choose this size of towers, most of the back-to-back hits will indeed pass near the Interaction point and so hopefully through the pixel detector. For the larger towers, the efficiency would be lower, as there would be quite a lot back-to-back hits not going through the Pixel detector.

The other reason for choosing the smallest size of the tower is technical - with the size of the tower there is increase in noise. Because this increase is bigger than the increase in the event rate, the 0.1×0.1 towers have the best signal to noise ratio.

Next question is the size of the energy threshold. S. Zenz in [34] concludes, that the ideal threshold is 1.5 GeV deposited in the calorimeter in both crossings. This could rule out all extraordinary events when muon scatters somewhere in the detector. This is consistent with our simulation: Figure 4.27 shows the number of hits as a function of energy - we can see that the muons with the energy lower than 1 or 2 GeV mostly do not have enough hits to be properly
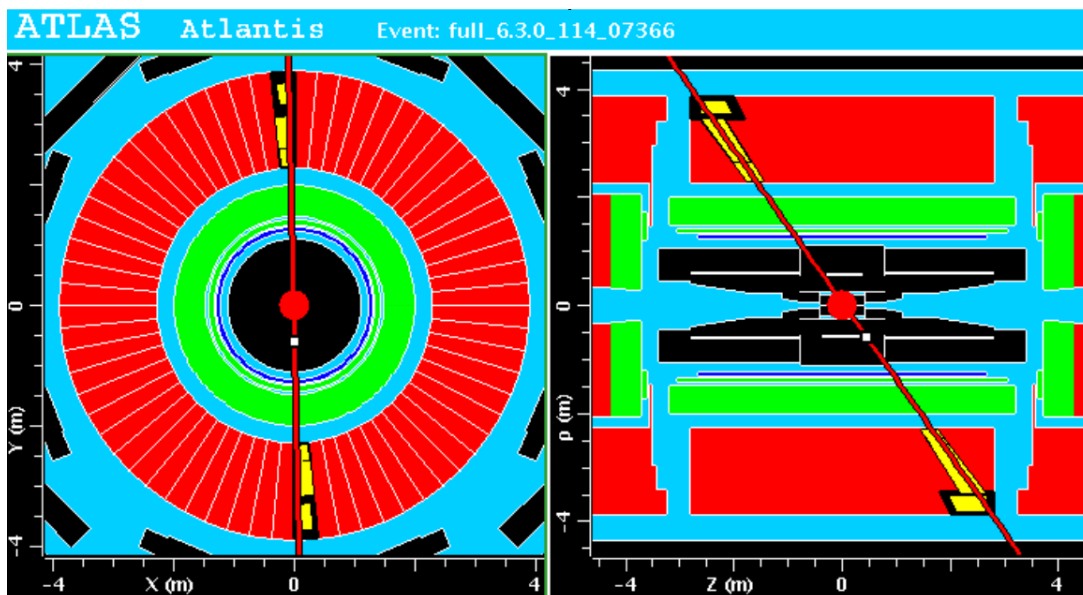
Figure 4.26: View of the ideal cosmic event, passing "back-to-back" through Tile calorimeter and the Pixel detector. Figure was made by Atlantis event view and is from [34].

reconstructed. The expected rate in [34] for the smallest towers and the energy cut at 1.5 GeV is 0.037 Hz[3].

The study [34] was interested not only in possibility of triggering muons by the tile calorimeter, but also on their distribution in the detector. It is worth to mention that it was one of the first simulations which took into account the effect of the shafts. He also calculated η and ϕ distributions and got figures very similar to our Figures 4.11 and 4.12, meaning that the shafts indeed have significant effect on the cosmic muon distribution.

---

[3]Study [34] was concerned only in barrel area, so that the real rate would be somehow bigger as about half of the cosmic muons are coming from high η direction
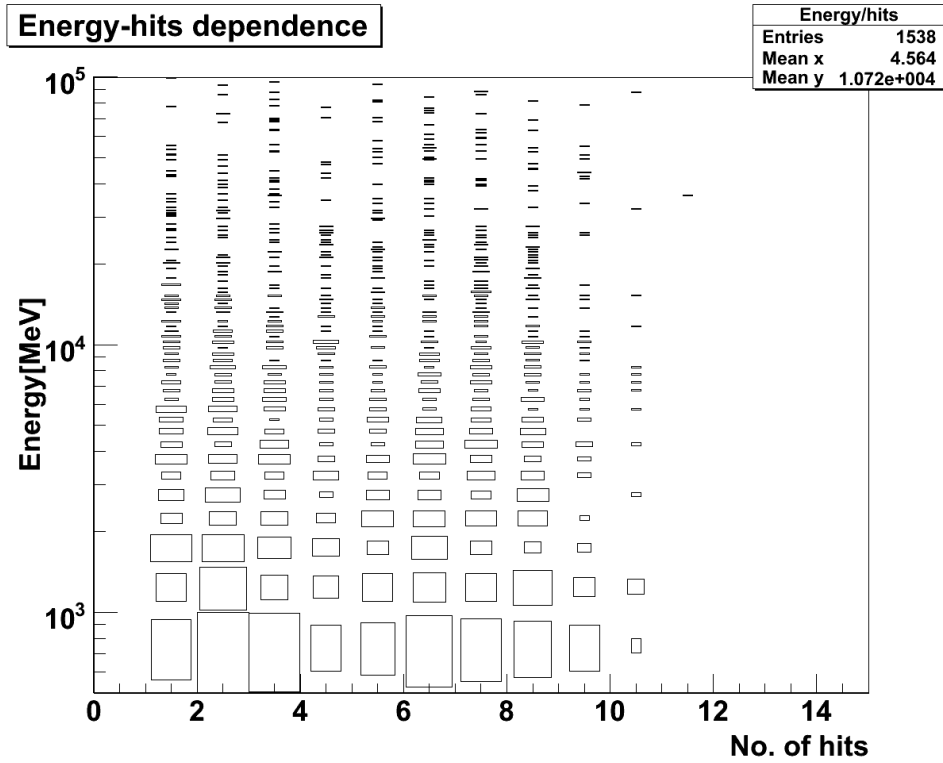
Figure 4.27: Energy of the first hit as the function of number of hits. It is based on data from *spec1* which contains a lot of low-energy muons. It shows that lowest energy moons have also the least hits, less than needed for proper reconstruction from Pixel data.

Chapter 5

Conclusions

In present, the particle physics is entering a very interesting period, comparable to the time when the Standard Model was born. Large Hadron collider will give us for the first time a real chance to completely validate the Standard model and/or find if there is something beyond it.

In particular, first task of LHC is finding the Higgs boson and measuring its properties. The way how to do it is of course different for various machines and Higgs masses. LHC and its experiments will have wide choice of discovery channels which together promise really large statistical significance of about 10 σ. This would mean, that the mass could be determined with a few GeV precision.

The LHC is also expected to give us clue for a "new physics" or "beyond the Standard model physics". There are various scenarios which try to deal with the questions Standard model cannot not answer. The most important ones are the Hierarchy problem and how neutrinos acquire mass (and also how big this mass is).

There are also other questions (number of free parameters, why do we have three families, etc.), but all these can be accommodated in the question whether there is a more fundamental theory than the Standard model and out present theory would be just its low energy limit. The LHC will surely not tell us how this theory look like, but it may very well tell if there is some and its basic shape.

Large Hadron Collider had truly large discovery potential and its results will be crucial in designing the International Linear Collider - powerful lepton collider which should come after LHC to do precise measurements in the areas of new discoveries.

The quality of the LHC answers will depend not only on the collider but also (and mostly) on its detectors. There are four big experiments on LHC and two of them are of general purpose design: CMS and ATLAS. Although they both have very similar aims they are designed differently, so that each of them will be good at something else. For example thanks to its calorimeters the CMS would be much more successful and precise in reconstructing Higgs boson from two photons (extremely clean, but also extremely rare channel).

ATLAS on the other hand has state-of-the-art tracking device both inner (Inner detector) and outer (Muon spectrometer). This means that it will have extraordinary performance for the final states with massive charged particles, like $H \to W^+W^-$. The most precise part of the ATLAS is the Pixel detector, which has two dimensional arrow of sensors and offer resolution 14 μm in polar angle ϕ direction and 87 μm in η direction.

The organic part of the HEP experiment is the computing, both online and offline. Every second trigger has to select few hundred events out of billions of others. To make this process as efficient as possible, the selection is done on three levels, every time increasing the amount of data involved. For offline ATLAS computing, there exists a software framework called Athena, which intends to simplify all programming and to give it a unit form. Although using Athena is far from trivial, it is now widespread and the ATLAS experimentalist use it almost exclusively

for all calculations.

One of the interesting problems in the ATLAS experiment is the question of cosmic rays - how big effect they will have and if they would be of any use. Because ATLAS will be ready several months before the LHC will start delivering the first beams, it is not an academic problem, but rather a very actual question because the cosmics will be the only data then.

To find a solution, we did a simulation within the Athena framework. That means that we had to generate billions of muons by Monte Carlo generator and then simulate their tracks in ATLAS and overburden by Geant4. We were particularly interested in the effect on the Pixel detector which forced us to add our own code to the simulation. Its purpose was to identify the muons hitting the Pixel detector and then write down their properties. The results of the simulation were subsequently analyzed by ROOT.

We found out that the pure hit rate of cosmic muons would be of order 1 Hz, which promises quite a lot of data for commissioning and alignment of the detector. Because of the ATLAS cavern geometry the cosmic hits will not be homogenously distributed as one would expect on the surface - it would be distorted by the presence of the large access shafts. Basically they allow large amounts of slow muons enter the cavern.

During an hour or so, all pixel modules in the barrel and most modules on the endcap discs will acquire at least one hit. Their position and energy distribution is remarkably uniform. What is even more important, the muons hitting Pixel detector fly almost straight. Both these facts could be well used in alignment. Although the cosmic measurement cannot give more precise results than the physical survey, it is an important independent test of the official alignment constants.

All our results were published and regularly presented on our group meetings [35–39].

This study is still ongoing and the actual problem is the form of cosmic trigger and its rate. The most promising is triggering by tile calorimeter, which yields (according to some previous study) the rate of about 100 events in Pixel barrel per hour which is perfectly consistent with our results.

Bibliography

[1] J. Hořejší, *Fundamentals of Electroweak Theory*, Karolinum Press, 2002

[2] J. Chýla, *Quarks, partons and Quantum Chromodynamics*, lecture notes, `http://www-hep2.fzu.cz/Theory/notes/text.pdf`

[3] Y. Dokshitzer, V. Khoze, A. Mueller and S. Troyan, *Basics of QCD*, Gif-sur-Yvette, France: Ed. Frontieres, 1991

[4] M. E. Peskin, D. V. Schroeder, *Introduction to quantum field theory*, Westview Press, 1995

[5] L. H. Ryder, *Quantum Field Theory*, 2nd edition, Cambridge University Press, 1996

[6] The LEP Collaborations, *A Combination of Preliminary Electroweak Measurements and Constraints on the Standard Model*, hep-ex/0612034v2

[7] M. Drees, *An Introduction to Supersymmetry*,hep-ph/9611409

[8] D. Rainwater, *Searching for the Higgs boson*, hep-ph/0702124v1

[9] J. Cammin, Ph.D. Thesis [ATLAS], BONN-IR-2004-06

[10] S. Asai et al., Eur. Phys. J. C 32S2, 19 (2004).

[11] F. Wilczek, *Higgs Portal into Hidden Sectors*, talk given at CERN on May 31, 2007; `http://indico.cern.ch/conferenceDisplay.py?confId=a07117`

[12] Phys. Rev. 159, 1251 - 1256 (1967)

[13] O. Piguet, *Introduction to Supersymmetric Gauge Theories*, hep-th/9710095

[14] CMS Outreach, `http://cmsinfo.cern.ch/`

[15] ALICE experiment: Panorama of ALICE, `http://aliceinfo.cern.ch/Public/panorama/`

[16] LHCb public pages, `http://lhcb-new.web.cern.ch/`

[17] LHC machine Outreach, `http://lhc-machine-outreach.web.cern.ch/lhc-machine-outreach/`

[18] ATLAS experiment public pages, `http://atlas.ch/`

[19] O. S. Brüning *et al.*, *LHC Design Report v.1*, CERN-2004-003-V-1,

[20] ATLAS collaboration, *ATLAS Technical Proposal for a General-Purpose pp Experiment at the Large Hadron Collider at CERN*, 2nd edition, CERN, 1994

[21] Atlantis event display homepage `http://www.hep.ucl.ac.uk/atlas/atlantis/`

[22] The LXR Cross-Referencer, `http://alxr.usatlas.bnl.gov/lxr/source`

[23] ATLAS Twiki homepage, `https://twiki.cern.ch/twiki/bin/view/Atlas/`

[24] Static ATLAS Offline software pages `http://atlas-computing.web.cern.ch/atlas-computing/computing.php`

[25] Athena code Doxygen documentation `https://twiki.cern.ch/twiki/bin/view/Atlas/DoxygenDocumentation`

[26] CERN hypernews `https://hypernews.cern.ch/`

[27] ROOT framework homepage `http://root.cern.ch/`

[28] M.Boonekamp *et al.*, *Cosmic Ray, Beam-Halo and Beam-Gas Rate Studies for ATLAS Commissioning*, ATL-GEN-2004-001

[29] LHC commissioning web page `http://lhc-commissioning.web.cern.ch/lhc-commissioning/`

[30] ATLAS Pixel group, *Pixel Offline Analysis for EndcapA Cosmic Data*, note in preparation

[31] W.-M. Yao et al., Journal of Physics G 33, 1 (2006)

[32] Allkofer et al, Phys. Lett. 36B (1971), 425

[33] ATLAS detector simulation, online manual, `http://atlas-computing.web.cern.ch/atlas-computing/packages/simulation/geant4/geant4.html`

[34] S. Zenz, *Simulation of Cosmic Muons in the ATLAS Tile Calorimeter*, University of Chicago `http://hep.uchicago.edu/atlas/commissioning/Zenz.doc`

[35] P. Jež, *Towards cosmics with the pixel detector in the ATLAS cavern*, Pixel Offline Software Meeting, June 04, 2007, `http://indico.cern.ch/conferenceDisplay.py?confId=16452`

[36] P. Jež, *Cosmics*, Pixel Offline Software Meeting, June 18, 2007, `http://indico.cern.ch/conferenceDisplay.py?confId=17691`

[37] P. Jež, M. Marčišovský, *Calculation of the cosmic muon rate going through the pixel detector in the pit*, Pixel Offline Software Meeting, July 30, 2007, `http://indico.cern.ch/conferenceDisplay.py?confId=19451`

[38] P. Jež, M. Marčišovský, *Cosmic muon rate through pixel detector and muon distributions in the pit*, Pixel Offline Software Meeting, August 13, 2007, `http://indico.cern.ch/conferenceDisplay.py?confId=19596`

[39] M. Zeman*Commissioning activities*, Pixel Offline Software Meeting, August 27, 2007, `http://indico.cern.ch/conferenceDisplay.py?confId=20224`

[40] M. Scherzer,, *Hardware Blog: ATLAS*, `http://octopart.com/blog/get?y=2007&m=6&d=6`